PHYSICAL REVIEW D **92,** 035013 (2015)

Chromoelectric dipole moments of quarks in MSSM extensions

Amin Aboubrahim,[2,§] Tarek Ibrahim,[1,*] Pran Nath,[3,†] and Anas Zorik[4,‡]

[1]*University of Science and Technology, Zewail City of Science and Technology, 6th of October City, Giza 12588, Egypt*

[2]*Department of Physics, Faculty of Science, Beirut Arab University, Beirut 11-5020, Lebanon*

[3]*Department of Physics, Northeastern University, Boston, Massachusetts 02115-5000, USA*

[4]*Department of Physics, Faculty of Science, Alexandria University, Alexandria 21511, Egypt*

(Received 9 July 2015; published 19 August 2015)

An analysis is given of the chromoelectric dipole moment of quarks and of the neutron in an MSSM extension where the matter sector contains an extra vectorlike generation of quarks and mirror quarks. The analysis includes contributions to the chromoelectric dipole moment from the exchange of the W and the Z bosons, from the exchange of charginos and neutralinos and the gluino. Their contribution to the electric dipole moment (EDM) of quarks is investigated. The interference between the minimal supersymmetric standard model sector and the new sector with vectorlike quarks is investigated. It is shown that inclusion of the vectorlike quarks can modify the quark EDMs in a significant way. Further, this interference also provides a probe of the vectorlike quark sector. These results are of interest as in the future measurements on the neutron EDM could see an improvement up to 2 orders of magnitude over the current experimental limits and provide an instrument for a further probe of new physics beyond the standard model.

DOI: 10.1103/PhysRevD.92.035013 PACS numbers: 12.60.-i, 14.60.Fg

I. INTRODUCTION

New sources of CP violation beyond those that exist in the standard model are needed to explain baryogenesis and are also worthy of study in their own right as possible probes of beyond the standard model physics (for reviews see, e.g., Refs. [1–4]). Such sources can also induce an electric dipole moment in elementary particles which can be significantly larger than those expected in the standard model [1,2]. In this work we are specifically interested in the electric dipole moment (EDM) of the quarks arising from the chromoelectric dipole operator. Thus, the electroweak sector of the standard model produces an EDM which is 10^{-30} ecm [5–7], and it lies beyond the possibility of its observation in the foreseeable future. As mentioned in particle physics models beyond the standard model, it is possible to generate much larger values for the EDM. In this work we focus on one such model—an extension of the minimal supersymmetric standard model (MSSM) with a vectorlike multiplet [8]. Such an extension is anomaly free, and thus the nice quantum properties of the MSSM are maintained. Further, vectorlike multiplets arise in a variety of settings such as in grand unified models and in string and D brane models [8–10]. Vectorlike generations have been considered by several authors since their discovery would constitute new physics (see, e.g., Refs. [9–22]). Such models have new sources of CP violation and thus can generate substantial size dipole operators. For that reason they are interesting models to consider in the context of lepton and quark EDMs. In a recent work, we analyzed the electric dipole operator in such a setting [23], and in this work we analyze the chromoelectric dipole operator in the extended MSSM model and its contribution to the electric dipole moments.

Before discussing the EDM in the new class of models, it is relevant to recall the situation regarding the lepton and quark EDMs in the MSSM. Here it is well known that the MSSM has a supersymmetry (SUSY) CP problem, i.e., that the EDM predicted with SUSY phases $O(1)$ is typically in excess of the experimental upper limits. A number of remedies have been offered in the past to remedy this problem. These include a fine-tuning of the phases to be small [24]; suppression of the EDM by large sparticle masses [25]; suppression of the EDM where various contributions conspire to cancel, i.e., the cancellation mechanism [26,27]; as well as other possible remedies (see, e.g., Ref. [28]). It has also been suggested that the EDM be used as a probe of new physics beyond the standard model [18,29–32]. Specifically the experimental limits on the EDMs can be used as vehicles to probe a new physics regime not accessible otherwise to current and future detectors.

The outline of the rest of the paper is as follows. In Sec. II we give a brief description of the model and describe the nature of mixing between the vector generation and the standard three generations of quarks. In Sec. III. A we discuss the loop contributions to the

*Permanent address: Department of Physics, Faculty of Science, University of Alexandria, Alexandria 21511, Egypt. tibrahim@zewailcity.edu.eg

†nath@neu.edu

‡anas.zorik@alexU.edu.eg

§abouibrahim.a@husky.neu.edu

chromoelectric dipole moment of the up quark and the down quark that arise from the exchange of the W boson in the loop. In Sec. III. B we give an analysis similar to that of Sec. III. A for the exchange of the Z boson. In Sec. III. C we compute the contribution from the exchange of charginos in the loop, and in Sec. III. D a similar analysis for the exchange of neutralinos in the loop is given. Finally in Sec. III. E we give the analysis for the exchange of the gluino in the loop. In Sec. IV we discuss the method for the computation of the neutron dipole moment using the quark dipole moments. In Sec. V we give a detailed numerical analysis of the contributions to the quark chromoelectric dipole moment (CEDM) and to the neutron CEDM for a variety of parameter points in the extended MSSM model. Here we also discuss the use of the neutron EDM as a probe of high mass scales. Conclusions are given in Sec. VI. Further details of the calculational aspects of the analysis are given in Appendixes A–C.

II. MODEL

Here we briefly describe the model, and further details are given in the Appendix. The model we consider is an extension of the MSSM with an additional vectorlike multiplet. Like the MSSM the vectorlike extension is free of anomalies, and as discussed in the Introduction, vectorlike multiplets appear in a variety of settings which include grand unified models, string and D brane models. Here we focus on the quark sector where the vectorlike multiplet consists of a fourth generation of quarks and their mirror quarks. Thus, the quark sector of the extended MSSM model is given by Eqs. (1) and (2), where

$$q_{iL} \equiv \begin{pmatrix} t_{iL} \\ b_{iL} \end{pmatrix} \sim \left(3, 2, \frac{1}{6}\right); \qquad t^c_{iL} \sim \left(3^*, 1, -\frac{2}{3}\right); \qquad b^c_{iL} \sim \left(3^*, 1, \frac{1}{3}\right); \quad i = 1, 2, 3, 4. \tag{1}$$

$$Q^c \equiv \begin{pmatrix} B^c_L \\ T^c_L \end{pmatrix} \sim \left(3^*, 2, -\frac{1}{6}\right); \qquad T_L \sim \left(3, 1, \frac{2}{3}\right); \qquad B_L \sim \left(3^*, 1, -\frac{1}{3}\right). \tag{2}$$

The numbers in the braces show the properties under $SU(3)_C \times SU(2)_L \times U(1)_Y$ where the first two entries label the representations for $SU(3)_C$ and $SU(2)_L$ and the last one gives the value of the hypercharge normalized so that $Q = T_3 + Y$. We allow the mixing of the vectorlike generation with the first three generations. Specically the mixings of the vectorlike multiplet involves the mirrors as well as the fourth generation. Details of these mixings are given in Eq. (A1). Here we display some relevant features. In the up-quark sector, we choose a basis as

$$\bar{\xi}^T_R = (\,\bar{t}_R \quad \bar{T}_R \quad \bar{c}_R \quad \bar{u}_R \quad \bar{t}_{4R}\,), \qquad \xi^T_L = (\,t_L \quad T_L \quad c_L \quad u_L \quad \bar{t}_{4L}\,), \tag{3}$$

and we write the mass term so that

$$-\mathcal{L}^u_m = \bar{\xi}^T_R(M_u)\xi_L + \text{H.c.} \tag{4}$$

The interaction of Eq. (A1) leads to the up-quark mass matrix M_u which is given by

$$M_u = \begin{pmatrix} y'_1 v_2/\sqrt{2} & h_5 & 0 & 0 & 0 \\ -h_3 & y_2 v_1/\sqrt{2} & -h'_3 & -h''_3 & -h_6 \\ 0 & h'_5 & y'_3 v_2/\sqrt{2} & 0 & 0 \\ 0 & h''_5 & 0 & y'_4 v_2/\sqrt{2} & 0 \\ 0 & h_8 & 0 & 0 & y'_5 v_2/\sqrt{2} \end{pmatrix}. \tag{5}$$

This mass matrix is not Hermitian, and a biunitary transformation is needed to diagonalize it. Thus, one has

$$D^{u\dagger}_R(M_u)D^u_L = \text{diag}(m_{u_1}, m_{u_2}, m_{u_3}, m_{u_4}, m_{u_5}). \tag{6}$$

Under the biunitary transformations, the basis vectors transform so that

$$\begin{pmatrix} t_R \\ T_R \\ c_R \\ u_R \\ t_{4R} \end{pmatrix} = D_R^u \begin{pmatrix} u_{1_R} \\ u_{2_R} \\ u_{3_R} \\ u_{4_R} \\ u_{5_R} \end{pmatrix}, \qquad \begin{pmatrix} t_L \\ T_L \\ c_L \\ u_L \\ t_{4L} \end{pmatrix} = D_L^u \begin{pmatrix} u_{1_L} \\ u_{2_L} \\ u_{3_L} \\ u_{4_L} \\ u_{5_L} \end{pmatrix}. \tag{7}$$

A similar analysis can be carried out for the down quarks. Here we choose the basis set as

$$\bar{\eta}_R^T = (\,\bar{b}_R \quad \bar{B}_R \quad \bar{s}_R \quad \bar{d}_R \quad \bar{b}_{4R}\,), \qquad \eta_L^T = (\,b_L \quad B_L \quad s_L \quad d_L \quad b_{4L}\,). \tag{8}$$

In this basis the down-quark mass terms are given by

$$-\mathcal{L}_m^d = \bar{\eta}_R^T(M_d)\eta_L + \text{H.c.}, \tag{9}$$

where, using the interactions of Eq. (A1), M_d has the following form:

$$M_d = \begin{pmatrix} y_1 v_1/\sqrt{2} & h_4 & 0 & 0 & 0 \\ h_3 & y_2' v_2/\sqrt{2} & h_3' & h_3'' & h_6 \\ 0 & h_4' & y_3 v_1/\sqrt{2} & 0 & 0 \\ 0 & h_4'' & 0 & y_4 v_1/\sqrt{2} & 0 \\ 0 & h_7 & 0 & 0 & y_5 v_1/\sqrt{2} \end{pmatrix}. \tag{10}$$

In general $h_3, h_4, h_5, h_3', h_4', h_5', h_3'', h_4'', h_5'', h_6, h_7, h_8$ can be complex, and we define their phases so that

$$h_k = |h_k| e^{i\chi_k}, \qquad h_k' = |h_k'| e^{i\chi_k'}, \qquad h_k'' = |h_k''| e^{i\chi_k''}. \tag{11}$$

The squark sector of the model contains a variety of terms including F-type, D-type and SUSY soft breaking terms. The details of these contributions to squark mass square matrices are discussed in Appendix A.

III. ANALYSIS OF CHROMOELECTRIC DIPOLE MOMENT OPERATOR

The chromoelectric dipole moment $\tilde{d}^C$ is the coefficient of the effective dimension-5 operator which is defined by

$$\mathcal{L}_I = -\frac{i}{2}\tilde{d}_q^C \bar{q}\sigma_{\mu\nu}\gamma_5 T^a q G^{\mu\nu a}, \tag{12}$$

where $G^{\mu\nu a}$ is the gluon field strength and T^a are the $SU(3)$ generators. The quarks will have five different contributions to the CEDM arising from the W, Z, gluino, chargino and neutralino exchanges. We denote these contributions by $\tilde{d}_u^C(W)$, $\tilde{d}_u^C(Z)$, $\tilde{d}_u^C(\tilde{g})$, $\tilde{d}_u^C(\chi^+)$ and $\tilde{d}_u^C(\chi^0)$. We discuss each of these contributions below.

A. W-exchange contribution to the quark CEDM

For the up quark, the W-exchange contribution arises from the left diagram of Fig. 1 using the interaction of Eq. (13), i.e.,

$$-\mathcal{L}_{dWu} = W_\rho^\dagger \sum_{i=1}^{5}\sum_{j=1}^{5} \bar{u}_j \gamma^\rho [G_{L_{ji}}^W P_L + G_{R_{ji}}^W P_R] d_i + \text{H.c.}, \tag{13}$$

where G_L^W and G_R^W are defined in Appendix B. The contribution of the W-exchange graph to $\tilde{d}_u^C$ is given by

$$\tilde{d}_u^C(W) = \frac{g_s}{16\pi^2}\sum_{i=1}^{5}\frac{m_{d_i}}{m_W^2}\text{Im}(G_{L4i}^W G_{R4i}^{W*}) I_1\left(\frac{m_{d_i}^2}{m_W^2}, \frac{m_{u_4}^2}{m_W^2}\right), \tag{14}$$

where $I_1(r_1, r_2)$ is a form factor given by

$$I_1(r_1, r_2) = \int_0^1 dx \frac{(4 + r_1 - r_2)x - 4x^2}{1 + (r_1 - r_2 - 1)x + r_2 x^2}. \tag{15}$$

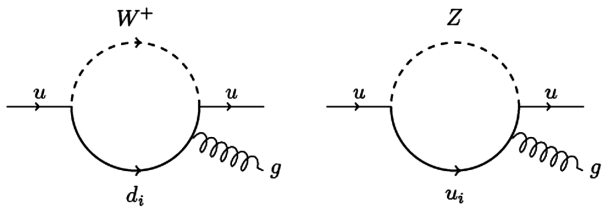

FIG. 1. W- and Z-exchange contributions to the CEDM of the up quark. Similar exchange contributions exist for the CEDM of the down quark where u and d are interchanged and W^+ is replaced by W^- in the diagrams above.

In the limit when r_2 is very small as is the case here, this integral gives the closed form

$$I_1(r_1,0)=\frac{2}{(1-r_1)^2}\left[1+\frac{1}{4}r_1+\frac{1}{4}r_1^2+\frac{3r_1\ln r_1}{2(1-r_1)}\right]. \quad (16)$$

The W contribution to the down-quark CEDM is given by

$$\tilde{d}_d^C(W)=\frac{g_s}{16\pi^2}\sum_{i=1}^{5}\frac{m_{u_i}}{m_W^2}\mathrm{Im}(G_{Li4}^{W*}G_{Ri4}^{W})I_1\left(\frac{m_{u_i}^2}{m_W^2},\frac{m_{d_4}^2}{m_W^2}\right). \quad (17)$$

B. Z-exchange contribution to the quark CEDM

For the Z boson exchange, the interactions that enter with the up-type quarks are given by

$$-\mathcal{L}_{uuZ}=Z_\rho\sum_{j=1}^{5}\sum_{i=1}^{5}\bar{u}_j\gamma^\rho[C_{L_{ji}}^{uZ}P_L+C_{R_{ji}}^{uZ}P_R]u_i, \quad (18)$$

where the couplings C_L^{uZ} and C_R^{uZ} are defined in Appendix B. Using this interaction the computation of the Z-exchange contributions to the up quarks is given by the loop diagram to the right in Fig. 1. Its contribution is

$$\tilde{d}_u^C(Z)=\frac{g_s}{16\pi^2}\sum_{i=1}^{5}\frac{m_{u_i}}{m_Z^2}\mathrm{Im}(C_{L_{4i}}^{uZ}C_{R_{4i}}^{uZ*})I_1\left(\frac{m_{u_i}^2}{m_Z^2},\frac{m_{u_4}^2}{m_Z^2}\right). \quad (19)$$

For the Z boson exchange, the interactions that enter with the down-type quarks are given by

$$-\mathcal{L}_{ddZ}=Z_\rho\sum_{j=1}^{5}\sum_{i=1}^{5}\bar{d}_j\gamma^\rho[C_{L_{ji}}^{dZ}P_L+C_{R_{ji}}^{dZ}P_R]d_i, \quad (20)$$

where the couplings C_L^{dZ} and C_R^{dZ} are as defined in Appendix B. A calculation similar to that of the up-quark CDEM gives a contribution to the d-quark moment so that

$$\tilde{d}_d^C(Z)=\frac{g_s}{16\pi^2}\sum_{i=1}^{5}\frac{m_{d_i}}{m_Z^2}\mathrm{Im}(C_{L_{4i}}^{dZ}C_{R_{4i}}^{dZ*})I_1\left(\frac{m_{d_i}^2}{m_Z^2},\frac{m_{d_4}^2}{m_Z^2}\right). \quad (21)$$

C. Chargino exchange contribution to the CEDM

In this section we discuss the interactions in the mass diagonal basis involving squarks, charginos and quarks. Thus, we have

$$-\mathcal{L}_{u-\tilde{d}-\chi^-}=\sum_{j=1}^{5}\sum_{i=1}^{2}\sum_{k=1}^{10}\bar{u}_j(C_{jik}^{Lu}P_L+C_{jik}^{Ru}P_R)\tilde{\chi}^{ci}\tilde{d}_k+\mathrm{H.c.}, \quad (22)$$

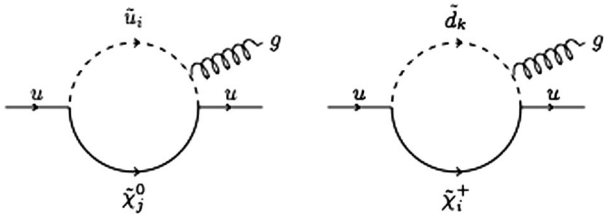

FIG. 2. Left diagram: Supersymmetric loop contributions to the CEDM of the up quark from the diagram involving the exchange of neutralinos and up squarks. Right diagram: Chargino and down-squark loop contribution to the CEDM of the up quark. Similar loop contributions exist for the CEDM of the down quark, where u and d are interchanged, $\tilde{u}$ and $\tilde{d}$ are interchanged, and χ^+ is replaced by χ^- in the diagrams above.

and

$$-\mathcal{L}_{d-\tilde{u}-\chi^-}=\sum_{j=1}^{5}\sum_{i=1}^{2}\sum_{k=1}^{10}\bar{d}_j(C_{jik}^{Ld}P_L+C_{jik}^{Rd}P_R)\tilde{\chi}^{ci}\tilde{u}_k+\mathrm{H.c.}, \quad (23)$$

where the couplings C^{Lu}, C^{Ru}, C^{Ld} and C^{Rd} and are as defined in Appendix B. The loop contributions to the up-quark CEDM arise from the right diagram of Fig. 2. Their contribution to the CEDM of quarks using Eqs. (22) and (23) are given by

$$\tilde{d}_u^C(\chi^+)=\frac{g_s}{16\pi^2}\sum_{i=1}^{2}\sum_{k=1}^{10}\frac{m_{\chi_i^+}}{M_{\tilde{d}_k}^2}\mathrm{Im}(C_{4ik}^{Lu}C_{4ik}^{Ru*})I_3\left(\frac{m_{\chi_i^+}^2}{M_{\tilde{d}_k}^2},\frac{m_{u_4}^2}{M_{\tilde{d}_k}^2}\right), \quad (24)$$

$$\tilde{d}_d^C(\chi^+)=\frac{g_s}{16\pi^2}\sum_{i=1}^{2}\sum_{k=1}^{10}\frac{m_{\chi_i^+}}{M_{\tilde{u}_k}^2}\mathrm{Im}(C_{4ik}^{Ld}C_{4ik}^{Rd*})I_3\left(\frac{m_{\chi_i^+}^2}{M_{\tilde{u}_k}^2},\frac{m_{d_4}^2}{M_{\tilde{u}_k}^2}\right), \quad (25)$$

where $I_3(r_1,r_2)$ is given by

$$I_3(r_1,r_2)=\int_0^1 dx\frac{x-x^2}{1+(r_1-r_2-1)x+r_2x^2}. \quad (26)$$

In the limit when r_2 is very small as is the case here, we have the closed form

$$I_3(r_1,0)=\frac{1}{2(r_1-1)^2}\left(1+r_1+\frac{2r_1\ln r_1}{1-r_1}\right). \quad (27)$$

D. Neutralino exchange contribution to the CEDM

We now discuss the interactions in the mass diagonal basis involving up quarks, up squarks and neutralinos. Thus, we have

$$-\mathcal{L}_{u-\tilde{u}-\chi^0} = \sum_{i=1}^{5}\sum_{j=1}^{4}\sum_{k=1}^{10} \bar{u}_i (C'^L_{uijk} P_L + C'^R_{uijk} P_R)\tilde{\chi}^0_j \tilde{u}_k + \text{H.c.} \tag{28}$$

The interaction of the down quarks, down squarks and neutralinos is given by

$$-\mathcal{L}_{d-\tilde{d}-\chi^0} = \sum_{i=1}^{4}\sum_{j=1}^{4}\sum_{k=1}^{10} \bar{d}_i (C'^L_{dijk} P_L + C'^R_{dijk} P_R)\tilde{\chi}^0_j \tilde{d}_k + \text{H.c.}, \tag{29}$$

where the couplings C'^L and C'^R as given in Appendix B. Using the interactions of Eq. (28), the neutralino exchange contribution to the CEDM of the up quark is given by

$$\tilde{d}^C_u(\chi^0) = \frac{g_s}{16\pi^2}\sum_{i=1}^{4}\sum_{k=1}^{10}\frac{m_{\chi^0_i}}{M^2_{\tilde{u}_k}}\text{Im}(C'^L_{u4ik}C'^{R*}_{u4ik}) I_3\left(\frac{m^2_{\chi^0_i}}{M^2_{\tilde{u}_k}}, \frac{m^2_{u_4}}{M^2_{\tilde{u}_k}}\right). \tag{30}$$

Similarly using the interactions of Eq. (29), the CEDM of the down quark is given by

$$\tilde{d}^C_d(\chi^0) = \frac{g_s}{16\pi^2}\sum_{i=1}^{4}\sum_{k=1}^{10}\frac{m_{\chi^0_i}}{M^2_{\tilde{d}_k}}\text{Im}(C'^L_{d4ik}C'^{R*}_{d4ik}) I_3\left(\frac{m^2_{\chi^0_i}}{M^2_{\tilde{d}_k}}, \frac{m^2_{d_4}}{M^2_{\tilde{d}_k}}\right). \tag{31}$$

E. Gluino exchange contribution to the CEDM

$$-\mathcal{L}_{qq\tilde{g}} = \sqrt{2} g_s \sum_{j=1}^{3}\sum_{k=1}^{3}\sum_{a=1}^{8}\sum_{l=1}^{5}\sum_{m=1}^{10} T^a_{jk}\bar{q}^j_l \times [C_{L_{lm}} P_L + C_{R_{lm}} P_R]\tilde{g}_a \tilde{q}^k_m + \text{H.c.}, \tag{32}$$

where the couplings $C_{L_{lm}}$ and $C_{R_{lm}}$ are defined in Appendix B. Using Eq. (32) the gluino exchange contribution to the up-quark CEDM arising from the loop diagrams of Fig. 3 is given by

$$\tilde{d}^C_u(\tilde{g}) = \frac{g_s\alpha_s}{12\pi^2}\sum_{m=1}^{10}\frac{m_{\tilde{g}}}{M^2_{\tilde{u}_m}}\text{Im}(K_{L_{um}}K^*_{R_{um}}) I_5\left(\frac{m^2_{\tilde{g}}}{M^2_{\tilde{u}_m}}, \frac{m^2_{u4}}{M^2_{\tilde{u}_m}}\right). \tag{33}$$

Similarly using Eq. (32) the gluino contribution to the down-quark CEDM is given by

$$\tilde{d}^C_d(\tilde{g}) = \frac{g_s\alpha_s}{12\pi^2}\sum_{m=1}^{10}\frac{m_{\tilde{g}}}{M^2_{\tilde{d}_m}}\text{Im}(K_{L_{dm}}K^*_{R_{dm}}) I_5\left(\frac{m^2_{\tilde{g}}}{M^2_{\tilde{d}_m}}, \frac{m^2_{d4}}{M^2_{\tilde{d}_m}}\right). \tag{34}$$

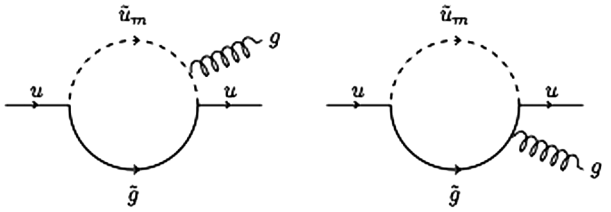

FIG. 3. Left diagram: Supersymmetric loop contributions to the CEDM of the up quark arising from the exchange of gluino and up squarks with the gluon emission from the internal up-squark line. Right diagram: Same as the left diagram except that the gluon emission is from the internal gluino line. Similar loop contributions exist for the CEDM of the down quark, where u and d are interchanged and $\tilde{u}$ and $\tilde{d}$ are interchanged.

Here $K_{L_{qm}}$ and $K_{R_{qm}}$ are given by

$$K_{L_{qm}} = (D^{q*}_{R24}\tilde{D}^q_{4m} - D^{q*}_{R54}\tilde{D}^q_{10m} - D^{q*}_{R44}\tilde{D}^q_{8m} - D^{q*}_{R34}\tilde{D}^q_{6m} - D^{q*}_{R14}\tilde{D}^q_{3m})e^{-i\xi_3/2}, \tag{35}$$

and

$$K_{R_{qm}} = (D^{q*}_{L44}\tilde{D}^q_{7m} + D^{q*}_{L54}\tilde{D}^q_{9m} + D^{q*}_{L34}\tilde{D}^q_{5m} + D^{q*}_{L14}\tilde{D}^q_{1m} - D^{q*}_{L24}\tilde{D}^q_{2m})e^{i\xi_3/2}, \tag{36}$$

where $I_5(r_1, r_2)$ is the loop function defined by

$$I_5(r_1, r_2) = \int_0^1 dx \frac{x + 8x^2}{1 + (r_1 - r_2 - 1)x + r_2 x^2}. \tag{37}$$

In the limit where r_2 is very small as is the case here, we get the closed form

$$I_5(r_1, 0) = \frac{1}{2(r_1 - 1)^2}\left(10r_1 - 26 + \frac{2r_1 \ln r_1}{1 - r_1} - \frac{18 \ln r_1}{1 - r_1}\right). \tag{38}$$

IV. NEUTRON CEDM

As discussed in the previous section, the total contribution to the CEDM of the quarks consists of five contributions arising from the exchange of the W, the Z, the charginos, the neutralinos and the gluino, so that

$$\tilde{d}^C_q = \tilde{d}^C_q(W) + \tilde{d}^C_q(Z) + \tilde{d}^C_q(\chi^+) + \tilde{d}^C_q(\chi^0) + \tilde{d}^C_q(\tilde{g}), \quad q = u, d. \tag{39}$$

The contribution of the chromoelectric operator to the EDMs of quarks can be computed using dimensional analysis [33]. The contribution to the quark EDM arising from $\tilde{d}^C_q$ is given by

$$d_q^C = \frac{e}{4\pi}\eta^C \tilde{d}_q^C, \tag{40}$$

where η^C is approximately equal to 3.4. The factor η^C brings the electric dipole moment from the electroweak scale down to the hadronic scale where it can be compared with the experiment. To obtain the contribution to the neutron EDM from the quark EDM, we use the nonrelativistic $SU(6)$ quark model which gives

$$d_n^C = \frac{1}{3}[4d_d^C - d_u^C]. \tag{41}$$

V. NUMERICAL ANALYSIS OF NEUTRON EDM

The current experimental limit on the EDM of the neutron is [34]

$$|d_n| < 2.9 \times 10^{-26}\ e\text{cm} \quad (90\%\ \text{C.L.}). \tag{42}$$

It is expected that a higher sensitivity by as much as 2 orders of magnitude more sensitive than the current limit may be achievable in the future [35].

We present now a numerical analysis of the neutron CEDM first for the case of the MSSM and next for the MSSM extension. The first analysis involves no mixing with the mirror generation and with the fourth sequential generation, and the only CP phases that appear are those from the MSSM sector. Thus, in this case all the mixing parameters, given in Eq. (11), are set to zero. The second analysis is for the MSSM extension where the mixings of the mirror generation and of the fourth sequential generation with the three generations are switched on. The results are given in Table II and Figs. 4–11. In the analysis in the squark sector, we assume $m_0^{u^2} = M_{\tilde{T}}^2 = M_{\tilde{t}_1}^2 = M_{\tilde{t}_2}^2 = M_{\tilde{t}_3}^2$ and $m_0^{d^2} = M_{\tilde{1}L}^2 = M_{\tilde{B}}^2 = M_{\tilde{b}_1}^2 = M_{\tilde{Q}}^2 = M_{\tilde{2}L}^2 = M_{\tilde{b}_2}^2 = M_{\tilde{3}L}^2 = M_{\tilde{b}_3}^2$. To simplify the numerical analysis further, we assume $m_0^u = m_0^d = m_0$. Additionally the trilinear couplings are chosen so that: $A_0^u = A_t = A_T = A_c = A_u = A_{4t}$ and $A_0^d = A_b = A_B = A_s = A_d = A_{4b}$. The input parameters are such that the sparticle spectrum that enters the loop is consistent with the current experimental limits from the LHC in each of the cases, i.e., with or without mixing.

We discuss now in further detail the cases without and with mixing with the vectorlike generation. We begin with the case with no mixing. In Table I, we give the individual contributions to the up- and down-quark EDM and CEDM, namely, the chargino, the neutralino and the gluino contributions. The W and Z contributions are not shown since they are absent in this case of no mixing with the vectorlike generation and the fourth sequential generation. The different contributions are given for two benchmark points (i) and (ii), where in the first the neutron EDM dominates the neutron CEDM and in the second the opposite is the case. The chargino and gluino contributions are the main contributors, while the neutralino contribution is suppressed. Note that the total neutron EDM, $|d_n|$, obtained by adding d_n^E and d_n^C in the table satisfy Eq. (42). Another observation is the largeness of the down-quark contribution in comparison with its up-quark counterpart. This is attributed to the large value of $\tan\beta$ which tends to enhance the down-quark couplings.

Next we consider the case with mixings. The results are presented in Table II for two benchmark points (i) and (ii). Here, in addition to the chargino, the neutralino and the gluino exchanges, one also has W and Z exchanges. The analysis shows the dominance of the EDM over the CEDM

TABLE I. An exhibition of the chargino, neutralino and gluino exchange contributions to the quark and the neutron EDM, CEDM and their sum for the case when there is no mixing of the vectorlike generation with the three generations. The analysis is for two benchmark points (i) and (ii). Benchmark (i): $\theta_\mu = 3.3 \times 10^{-3}$, $\xi_3 = 1 \times 10^{-3}$. Benchmark (ii): $\theta_\mu = 4.7 \times 10^{-3}$, $\xi_3 = 3.6$. The common parameters are $\tan\beta = 40$, $m_0 = m_0^u = m_0^d = 3000$, $|m_1| = 185$, $|m_2| = 220$, $|A_0^u| = 680$, $|A_0^d| = 600$, $|\mu| = 400$, $m_g = 1000$, $|h_3| = |h_3'| = |h_3''| = |h_4| = |h_4'| = |h_4''| = |h_5| = |h_5'| = |h_5''| = |h_6| = |h_7| = |h_8| = 0$, $\xi_1 = 2 \times 10^{-2}$, $\xi_2 = 2 \times 10^{-3}$, $\alpha_{A_0^u} = 2 \times 10^{-2}$, $\alpha_{A_0^d} = 3$. All masses are in GeV, all phases in rad, and the electric dipole moment in $e$cm.

	(i)		(ii)	
Contribution	Up	Down	Up	Down
Chargino, $d_q^{\chi^\pm}$	2.49×10^{-29}	-1.29×10^{-26}	2.16×10^{-29}	-2.08×10^{-26}
Neutralino, $d_q^{\chi^0}$	-2.49×10^{-32}	4.75×10^{-29}	-2.90×10^{-32}	5.47×10^{-29}
Gluino, d_q^g	3.42×10^{-29}	-4.24×10^{-28}	7.49×10^{-28}	2.06×10^{-26}
Total, d_q	5.90×10^{-29}	-1.32×10^{-26}	7.71×10^{-28}	-1.42×10^{-28}
EDM, d_n^E	-2.70×10^{-26}		-6.83×10^{-28}	
Chargino, $d_q^C(\chi^\pm)$	-3.41×10^{-30}	-2.15×10^{-27}	-2.89×10^{-30}	-3.40×10^{-27}
Neutralino, $d_q^C(\chi^0)$	-4.54×10^{-32}	-1.73×10^{-28}	-5.30×10^{-32}	-2.00×10^{-28}
Gluino, $d_q^C(\tilde{g})$	5.51×10^{-29}	1.37×10^{-27}	1.21×10^{-27}	-6.63×10^{-26}
Total, d_q^C	1.40×10^{-29}	-2.58×10^{-28}	3.26×10^{-28}	-1.89×10^{-26}
CEDM, d_n^C	-3.49×10^{-28}		-2.53×10^{-26}	

TABLE II. An exhibition of the chargino, neutralino, gluino, W- and Z-exchange contributions to the quark and the neutron EDM, CEDM and their sum for the case when there is mixing of the vectorlike generation with the three generations. The analysis is for two benchmark points (i) and (ii). Benchmark (i): $\theta_\mu = 4\times10^{-3}$, $\xi_3 = 1.12$. Benchmark (ii): $\theta_\mu = 4.6\times10^{-3}$, $\xi_3 = 4.71$. The common parameters are $\tan\beta = 40$, $m_0 = m_0^u = m_0^d = 5500$, $|m_1| = 185$, $|m_2| = 220$, $|A_0^u| = 680$, $|A_0^d| = 600$, $|\mu| = 400$, $m_g = 1100$, $m_T = 300$, $m_B = 240$, $m_{4t} = 320$, $m_{4b} = 280$, $|h_3| = 1.58$, $|h_3'| = 6.34\times10^{-2}$, $|h_3''| = 1.97\times10^{-2}$, $|h_4| = 4.42$, $|h_4'| = 5.07$, $|h_4''| = 12.87$, $|h_5| = 6.6$, $|h_5'| = 2.67$, $|h_5''| = 1.86\times10^{-1}$, $|h_6| = 1000$, $|h_7| = 1000$, $|h_8| = 1000$, $\xi_1 = 2\times10^{-2}$, $\xi_2 = 2\times10^{-3}$, $\alpha_{A_0^u} = 2\times10^{-2}$, $\alpha_{A_0^d} = 3$, $\chi_3 = 2\times10^{-2}$, $\chi_3' = 1\times10^{-3}$, $\chi_3'' = 4\times10^{-3}$, $\chi_4 = 7\times10^{-3}$, $\chi_4' = \chi_4'' = 1\times10^{-3}$, $\chi_5 = 9\times10^{-3}$, $\chi_5' = 5\times10^{-3}$, $\chi_5'' = 2\times10^{-3}$, $\chi_6 = \chi_7 = \chi_8 = 5\times10^{-3}$. All masses are in GeV, all phases in rad, and the electric dipole moment in $e$cm.

	(i)		(ii)	
Contribution	Up	Down	Up	Down
Chargino, $d_q^{\chi^\pm}$	7.65×10^{-30}	-6.91×10^{-27}	7.08×10^{-30}	-8.27×10^{-27}
Neutralino, $d_q^{\chi^0}$	3.93×10^{-32}	6.90×10^{-30}	3.91×10^{-32}	7.32×10^{-30}
Gluino, d_q^g	-2.01×10^{-28}	-5.35×10^{-27}	2.25×10^{-28}	5.91×10^{-27}
W Boson, d_q^W	3.77×10^{-30}	3.46×10^{-28}	3.77×10^{-30}	3.46×10^{-28}
Z Boson, d_q^Z	8.02×10^{-31}	3.05×10^{-29}	8.02×10^{-31}	3.05×10^{-29}
Total, d_q	-1.88×10^{-28}	-1.19×10^{-26}	2.37×10^{-28}	-1.97×10^{-27}
EDM, d_n^E	-2.41×10^{-26}		-4.13×10^{-27}	
Chargino, $d_q^C(\chi^\pm)$	-7.66×10^{-31}	-8.98×10^{-28}	-6.95×10^{-31}	-1.07×10^{-27}
Neutralino, $d_q^C(\chi^0)$	7.17×10^{-32}	-2.52×10^{-29}	7.14×10^{-32}	-2.68×10^{-29}
Gluino, $d_q^C(\tilde{g})$	-4.57×10^{-28}	2.44×10^{-26}	5.13×10^{-28}	-2.70×10^{-26}
W Boson, $d_q^C(W)$	-2.97×10^{-30}	2.29×10^{-28}	-2.97×10^{-30}	2.29×10^{-28}
Z Boson, $d_q^C(Z)$	1.46×10^{-30}	-1.11×10^{-28}	1.46×10^{-30}	-1.11×10^{-28}
Total, d_q^C	-1.24×10^{-28}	6.38×10^{-27}	1.38×10^{-28}	-7.56×10^{-27}
CEDM, d_n^C	8.54×10^{-27}		-1.01×10^{-26}	

for benchmark (i), while the opposite is the case for benchmark (ii). The total EDM for each benchmark point satisfies the experimental constraints of Eq. (42). Here we note that the EDM and CEDM are constrained not only by the experimental limits on the MSSM spectrum but also by the limits on new quarks. Thus, for the benchmarks presented in Table II, the vectorlike quarks have masses gotten by diagonalization of the matrices of Eqs. (5) and (10) and are given in Table III. The results of Table III are consistent with [36]. More stringent constraints on these masses will be available at the LHC RUN-II.

Next we give an analysis of the quark CEDMs' dependence on the mass scales as well as on the CP phases both in the MSSM sector as well as the new sector. Thus, the CEDM depends on the mass scale of the vectorlike sector, and in the MSSM sector, it depends on the universal scalar mass m_0 and on the gaugino mass scales. Further, it has dependence on several CP phases both from the MSSM sector as well as from the vectorlike sector. We discuss the

TABLE III. An exhibition of the masses of the heavy extra quarks corresponding to the parameter space of Table II.

Mirror up quark	$m_{t'} = 1037$ GeV
Mirror down quark	$m_{b'} = 740$ GeV
Fourth generation up quark	$m_4^{\rm up} = 1057$ GeV
Fourth generation down quark	$m_4^{\rm down} = 1260$ GeV

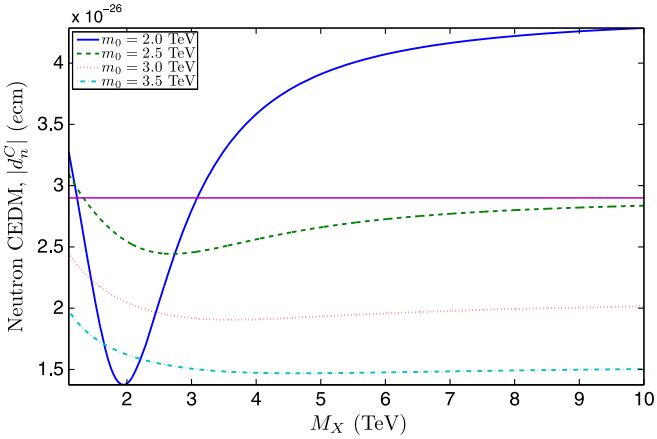

FIG. 4 (color online). Variation of the neutron CEDM $|d_n^C|$ vs M_X ($M_X = |h_6| = |h_7| = |h_8|$), for four values of m_0. From top to bottom at $M_X = 4$ TeV, $m_0 = m_0^u = m_0^d = 2.0$, 2.5, 3.0, 3.5 TeV. Other parameters have the values $\tan\beta = 14$, $|m_1| = 185$, $|m_2| = 220$, $|\mu| = 350$, $|A_0^u| = 680$, $|A_0^d| = 600$, $m_T = 300$, $m_B = 260$, $m_g = 1000$, $m_{4t} = 320$, $m_{4b} = 280$, $|h_3| = 1.58$, $|h_3'| = |h_3''| = RM_X$, $|h_4| = 4.42$, $|h_4'| = |h_4''| = RM_X$, $|h_5| = 6.6$, $|h_5'| = |h_5''| = RM_X$, $R = 1\times10^{-3}$, $\theta_\mu = 3.98$, $\xi_1 = \xi_2 = 4.52$, $\xi_3 = 2.42$, $\alpha_{A_0^u} = 5.0$, $\alpha_{A_0^d} = 1.14$, $\chi_3 = 2.38$, $\chi_3' = 4.92$, $\chi_3'' = 2.58$, $\chi_4 = 4.86$, $\chi_4' = 1.6$, $\chi_4'' = 1.37$, $\chi_5 = 1.14$, $\chi_5' = 4.39$, $\chi_5'' = 2.38$, $\chi_6 = 4.92$, $\chi_7 = 2.58$, $\chi_8 = 4.86$. All masses are in GeV, and phases are in rad.

dependence of the CEDM on the mass scales first and specifically on the mass scales M_X (from the vectorlike sector) and on m_0 and on m_g.

Figure 4 gives the dependence of the effect of the vectorlike generation on the CEDM where we exhibit the CEDM vs M_X, where $M_X = |h_6| = |h_7| = |h_8|$ and $|h_3'| = |h_3''| = |h_4'| = |h_4''| = |h_5'| = |h_5''| = RM_X$ while $R = 1 \times 10^{-3}$. We note that the allowed range of values for R is highly constrained. Thus, smaller values of R will not produce interesting results, while larger values are likely to upset the quark masses for the first three generations. The analysis shows that the CEDM lower than the upper limit can be obtained, and masses in the TeV range may be probed using the constraint given by Eq. (42) which should undergo further refinements in the future. The curve corresponding to $m_0 = 2$ TeV is characterized by a dip at $M_X \sim 1.9$ TeV. This dip quickly widens and is replaced by a shallow drop for $m_0 = 2.5$ TeV and then disappears completely for larger values of m_0. The variation of the CEDM eventually levels off for higher values of M_X and m_0. Further analysis shows that the dip is caused by a sudden drop in the mass of the lightest up-squark mass for $M_X \sim 1.9$ TeV in this region of the parameter space. The analysis of the dip is rather involved but arises as a result of the competition among the different components of the chromoelectric dipole moment operators, i.e, the W, Z, chargino, neutralino and gluino contributions. The analysis of Fig. 4 makes clear the very sensitive dependence of the CEDM on the vectorlike mass scale, and the exploration of this dependence is one of the primary motivations of this work.

Another way of looking at Fig. 4 is to plot the CEDM against m_0 for several values of M_X while R is fixed at 1×10^{-3} in the same region of parameter space. This is done in Fig. 5. The plot shows peaks between 2 and 3 TeV, and then the CEDM decreases gradually for increasing values of m_0. The peak is more pronounced for small values of M_X and disappears for larger values (for $M_X = 5$ TeV, here). The peaks occur in regions where m_0 and M_X are comparable in size as shown in this region. All values of the CEDM obtained in this region of the parameter space lie below the current upper limit.

In Fig. 4 we investigated the dependence of the CEDM on the vectorlike mass M_X and found that there is a very significant dependence of the CEDM on M_X. It is of interest also to examine if the EDM shows a similar dependence on M_X. In Fig. 6 we exhibit this dependence where $|d_n^E|$ is plotted against M_X for the same set of m_0 values as in Fig. 4. Again as in the case of the CEDM, we find that the EDM also has a sensitive dependence on M_X. We note here that the analysis of this work for the EDM is more general than the analysis of Ref. [23]. Thus, in

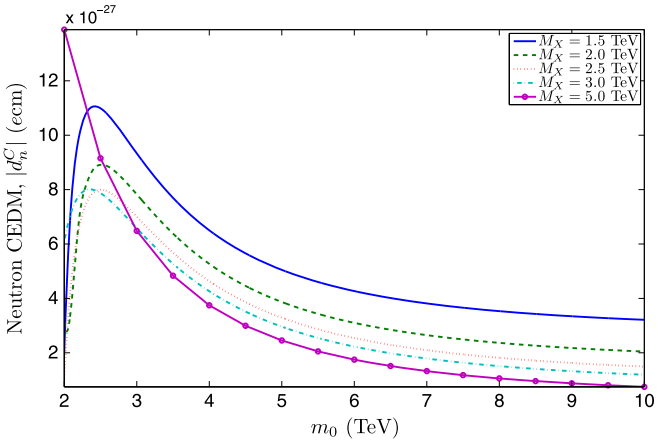

FIG. 5 (color online). Variation of the neutron CEDM $|d_n^C|$ vs the scalar mass m_0 ($m_0 = m_0^u = m_0^d$), for five values of M_X, ($M_X = |h_6| = |h_7| = |h_8|$). From top to bottom at $m_0 = 5$ TeV, $M_X = 1.5, 2.0, 2.5, 3.0, 5$ TeV. Other parameters have the values $\tan\beta = 14$, $|m_1| = 185$, $|m_2| = 220$, $|\mu| = 350$, $|A_0^u| = 680$, $|A_0^d| = 600$, $m_T = 300$, $m_B = 260$, $m_g = 1000$, $m_{4t} = 320$, $m_{4b} = 280$, $|h_3| = 1.58$, $|h_3'| = |h_3''| = RM_X$, $|h_4| = 4.42$, $|h_4'| = |h_4''| = RM_X$, $|h_5| = 6.6$, $|h_5'| = |h_5''| = RM_X$, $R = 1 \times 10^{-3}$, $\theta_\mu = 3.8$, $\xi_1 = \xi_2 = 4.52$, $\xi_3 = 2.42$, $\alpha_{A_0^u} = 5.0$, $\alpha_{A_0^d} = 1.14$, $\chi_3 = 2.38$, $\chi_3' = 4.92$, $\chi_3'' = 2.58$, $\chi_4 = 4.86$, $\chi_4' = 1.6$, $\chi_4'' = 1.37$, $\chi_5 = 1.14$, $\chi_5' = 4.39$, $\chi_5'' = 2.38$, $\chi_6 = 4.92$, $\chi_7 = 2.58$, $\chi_8 = 4.86$. All masses are in GeV, and phases are in rad.

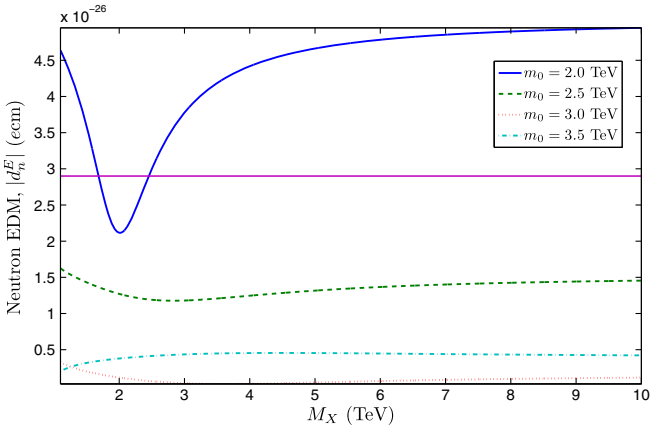

FIG. 6 (color online). Variation of the neutron EDM $|d_n^E|$ vs M_X ($M_X = |h_6| = |h_7| = |h_8|$), for four values of m_0. From top to bottom at $M_X = 1$ TeV, $m_0 = m_0^u = m_0^d = 2.0, 2.5, 3.0, 3.5$ TeV. Other parameters have the values $\tan\beta = 15$, $|m_1| = 185$, $|m_2| = 220$, $|\mu| = 350$, $|A_0^u| = 680$, $|A_0^d| = 600$, $m_T = 300$, $m_B = 260$, $m_g = 1000$, $m_{4t} = 320$, $m_{4b} = 280$, $|h_3| = 1.58$, $|h_3'| = |h_3''| = RM_X$, $|h_4| = 4.42$, $|h_4'| = |h_4''| = RM_X$, $|h_5| = 6.6$, $|h_5'| = |h_5''| = RM_X$, $R = 1 \times 10^{-3}$, $\theta_\mu = 5 \times 10^{-3}$, $\xi_1 = 2 \times 10^{-2}$, $\xi_2 = 2 \times 10^{-3}$, $\xi_3 = 4.0$, $\alpha_{A_0^u} = 2 \times 10^{-2}$, $\alpha_{A_0^d} = 3.0$, $\chi_3 = 2 \times 10^{-2}$, $\chi_3' = 1 \times 10^{-3}$, $\chi_3'' = 4 \times 10^{-3}$, $\chi_4 = 7 \times 10^{-3}$, $\chi_4' = \chi_4'' = 1 \times 10^{-3}$, $\chi_5 = 9 \times 10^{-3}$, $\chi_5' = 5 \times 10^{-3}$, $\chi_5'' = 2 \times 10^{-3}$, $\chi_6 = \chi_7 = \chi_8 = 5 \times 10^{-3}$. All masses are in GeV, and phases are in rad.

Ref. [23] we considered only the mixings of the three generations with the mirror generation so that the quark matrices were 4×4 and the squark square matrices were 8×8 and the parameter M_X did not appear in that work. On the other hand, in this work we are considering the mixing of the three generations with the full vectorlike generation consisting of the mirror and the sequential fourth generation. As a consequence the quark mass matrices are 5×5, and the squark mass squared matrices are 10×10, and this time we have also the dependence on the vectorlike mass M_X. Thus, the analysis of this work is more general than of the work of Ref. [23].

Next we study the dependence of the CEDM on the gluino mass. This is given in Figs. 7 and 8. Thus, in Fig. 7 the variation of the neutron CEDM, d_n^C, is plotted against the gluino mass, m_g. It is shown that CEDM values lower than the current experimental upper limit can be obtained in the given parameter space. The neutron CEDM decreases for increasing values of m_g but eventually levels off at around zero for some values of $\tan\beta$. However, for other values of $\tan\beta$, (e.g., $\tan\beta = 40$), the neutron CEDM levels off but turns negative. This phenomenon can be understood by analyzing different contributions to the CEDM as shown in Fig. 8. Specifically one finds that the negative contribution to the CEDM arises from the chargino exchange loop contribution, $d_d^c(\chi^\pm)$. Since we are not applying any grand unified theory constraints, the masses of the chargino

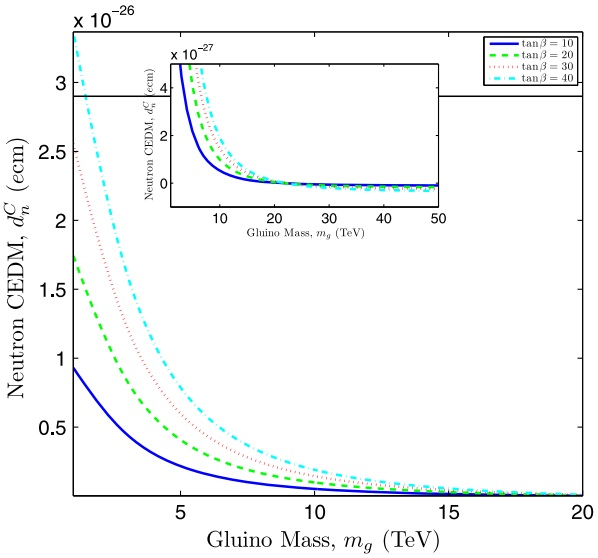

FIG. 7 (color online). Variation of the neutron CEDM d_n^C vs the gluino mass, m_g, for four values of $\tan\beta$. From bottom to top at $m_g = 5$ TeV, $\tan\beta = 10$, 20, 30, 40. Other parameters have the values $|m_1| = 170$, $|m_2| = 220$, $|\mu| = 450$, $|A_0^u| = 680$, $|A_0^d| = 600$, $m_0^u = m_0^d = 3700$, $m_T = 300$, $m_B = 260$, $m_{4t} = 320$, $m_{4b} = 280$, $|h_3| = 1.58$, $|h_3'| = 6.34 \times 10^{-2}$, $|h_3''| = 1.97 \times 10^{-2}$, $|h_4| = 4.42$, $|h_4'| = 5.07$, $|h_4''| = 2.87$, $|h_5| = 6.6$, $|h_5'| = 2.67$, $|h_5''| = 1.86 \times 10^{-1}$, $|h_6| = |h_7| = |h_8| = 1000$, $\theta_\mu = 2.6 \times 10^{-3}$, $\xi_1 = 2 \times 10^{-2}$, $\xi_2 = 2 \times 10^{-3}$, $\xi_3 = 1.6$, $\alpha_{A_0^u} = 2 \times 10^{-2}$, $\alpha_{A_0^d} = 3.0$, $\chi_3 = 2 \times 10^{-2}$, $\chi_3' = 1 \times 10^{-3}$, $\chi_3'' = 4 \times 10^{-3}$, $\chi_4 = 7 \times 10^{-3}$, $\chi_4' = \chi_4'' = 1 \times 10^{-3}$, $\chi_5 = 9 \times 10^{-3}$, $\chi_5' = 5 \times 10^{-3}$, $\chi_5'' = 2 \times 10^{-3}$, $\chi_6 = \chi_7 = \chi_8 = 5 \times 10^{-3}$. All masses are in GeV, and phases are in rad.

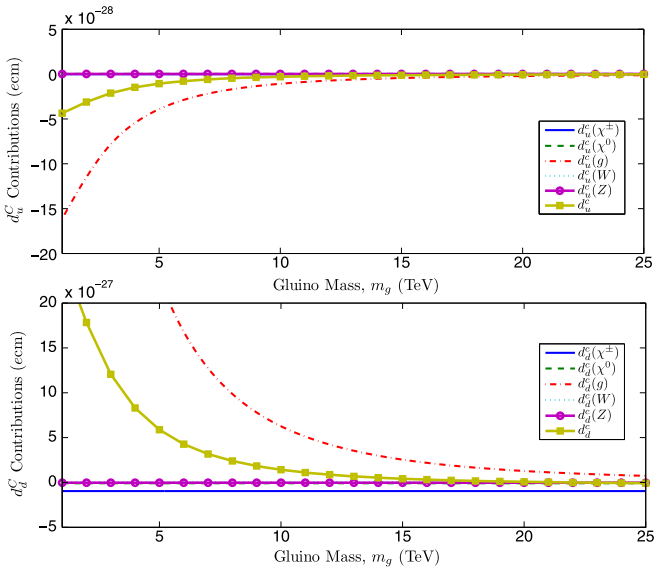

FIG. 8 (color online). Variation of up- and down-quark contributions to the neutron CEDM for $\tan\beta = 40$. Other parameters are the same as in Fig. 7.

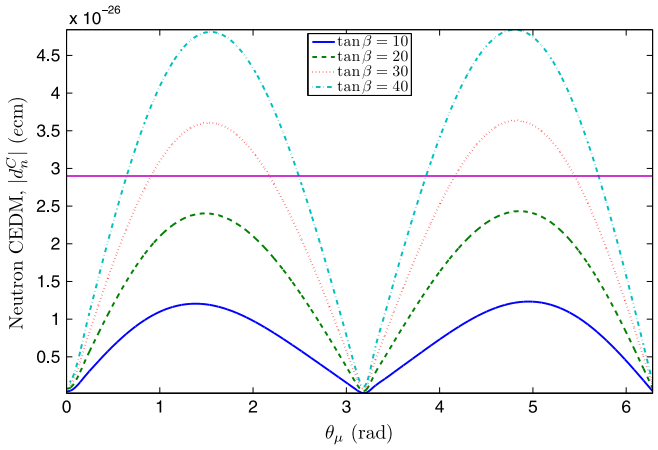

FIG. 9 (color online). Variation of the neutron CEDM $|d_n^C|$ vs θ_μ for four values of $\tan\beta$. From bottom to top at $\theta_\mu = 1$ rad, $\tan\beta = 10$, 20, 30, 40. Other parameters have the values $|m_1| = 170$, $|m_2| = 220$, $|\mu| = 400$, $|A_0^u| = 680$, $|A_0^d| = 600$, $m_0^u = m_0^d = 8000$, $m_g = 1000$, $m_T = 300$, $m_B = 260$, $m_{4t} = 320$, $m_{4b} = 280$, $|h_3| = 1.58$, $|h_3'| = 6.34 \times 10^{-2}$, $|h_3''| = 1.97 \times 10^{-2}$, $|h_4| = 4.42$, $|h_4'| = 5.07$, $|h_4''| = 2.87$, $|h_5| = 6.6$, $|h_5'| = 2.67$, $|h_5''| = 1.86 \times 10^{-1}$, $|h_6| = |h_7| = |h_8| = 1000$, $\xi_1 = 2 \times 10^{-2}$, $\xi_2 = 2 \times 10^{-3}$, $\xi_3 = 2.6$, $\alpha_{A_0^u} = 2 \times 10^{-2}$, $\alpha_{A_0^d} = 3.0$, $\chi_3 = 2 \times 10^{-2}$, $\chi_3' = 1 \times 10^{-3}$, $\chi_3'' = 4 \times 10^{-3}$, $\chi_4 = 7 \times 10^{-3}$, $\chi_4' = \chi_4'' = 1 \times 10^{-3}$, $\chi_5 = 9 \times 10^{-3}$, $\chi_5' = 5 \times 10^{-3}$, $\chi_5'' = 2 \times 10^{-3}$, $\chi_6 = \chi_7 = \chi_8 = 5 \times 10^{-3}$. All masses are in GeV, and phases are in rad.

and the gluino can be treated as independent parameters, and thus as we increase the gluino mass, the chargino contribution remains unchanged and eventually dominates as the gluino mass gets large and makes the CEDM negative for $m_g > 20$ TeV. We note here in passing that the W and Z contributions in this region of the parameter space are negligible compared to the other exchange contributions.

As discussed already, it is of interest to study the dependence of the CEDM on the *CP* phases in the MSSM sector as well as in the new sector. Figure 9 shows the variation of the neutron CEDM vs θ_μ, the phase of μ. The *CP* phases are the source of the CEDM, and the sensitivity that the CEDM shows in response to the variation of θ_μ is obvious. The parameter μ appears in the chargino and the neutralino mass matrices. It exists also in the squark mass squared matrices, so one can see that the chargino, the neutralino and the gluino contributions are affected by this parameter and its phase. The electroweak contributions, i.e, W and Z components, are independent of the magnitude and the phase of μ. Values of $|d_n^C|$ below the current upper limit can be obtained for several values of $\tan\beta$, whereas values above the limit appear for larger $\tan\beta$.

Next we investigate the dependence of the CEDM on χ_6 which explores a new sector of the theory as it is the *CP* phase that arises in interactions involving the mirror quarks

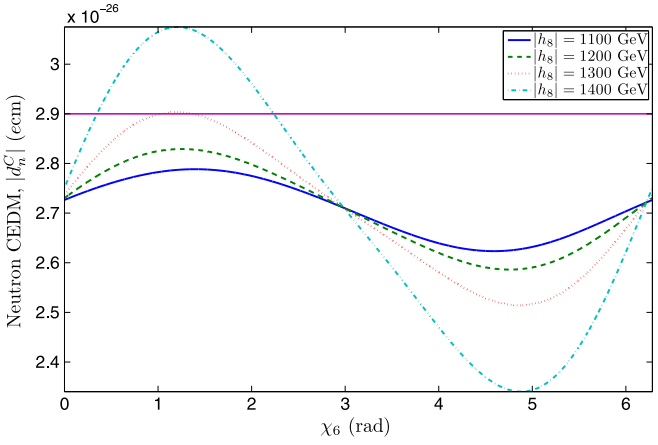

FIG. 10 (color online). Variation of the neutron CEDM $|d_n^C|$ vs χ_6, for four values of $|h_8|$. From bottom to top at $\chi_6 = 1$ rad, $|h_8| = 1100$, 1200, 1300, 1400 GeV. Other parameters have the values $\tan\beta = 34$, $|m_1| = 185$, $|m_2| = 220$, $|\mu| = 350$, $|A_0^u| = 680$, $|A_0^d| = 600$, $m_0^u = m_0^d = 3600$, $m_T = 300$, $m_B = 260$, $m_g = 4000$, $m_{4t} = 320$, $m_{4b} = 280$, $|h_3| = 1.58$, $|h_3'| = 6.34 \times 10^{-2}$, $|h_3''| = 1.97 \times 10^{-2}$, $|h_4| = 4.42$, $|h_4'| = 5.07$, $|h_4''| = 2.87$, $|h_5| = 6.6$, $|h_5'| = 2.67$, $|h_5''| = 1.86 \times 10^{-1}$, $|h_6| = |h_7| = 1100$, $\theta_\mu = 0.1$, $\xi_1 = 2 \times 10^{-2}$, $\xi_2 = 2 \times 10^{-3}$, $\xi_3 = 3.6$, $\alpha_{A_0^u} = 2 \times 10^{-2}$, $\alpha_{A_0^d} = 3.0$, $\chi_3 = 2 \times 10^{-2}$, $\chi_3' = 1 \times 10^{-3}$, $\chi_3'' = 4 \times 10^{-3}$, $\chi_4 = 7 \times 10^{-3}$, $\chi_4' = \chi_4'' = 1 \times 10^{-3}$, $\chi_5 = 9 \times 10^{-3}$, $\chi_5' = 5 \times 10^{-3}$, $\chi_5'' = 2 \times 10^{-3}$, $\chi_7 = \chi_8 = 5 \times 10^{-3}$. All masses are in GeV, and phases are in rad.

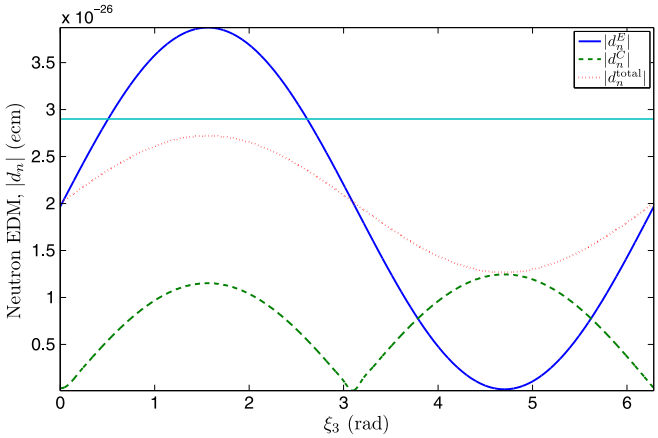

FIG. 11 (color online). Variation of the neutron EDM, $|d_n^E|$ (solid curve); the neutron CEDM, $|d_n^C|$ (dashed curve); and the total neutron EDM, $|d_n^{\text{total}}|$ (dotted curve) vs ξ_3, the phase of the gluino mass, for $\tan\beta = 40$. Other parameters have the values $|m_1| = 185$, $|m_2| = 220$, $|\mu| = 400$, $|A_0^u| = 680$, $|A_0^d| = 600$, $m_0^u = m_0^d = 5000$, $m_T = 300$, $m_B = 260$, $m_g = 1500$, $m_{4t} = 320$, $m_{4b} = 280$, $|h_3| = 1.58$, $|h_3'| = 6.34 \times 10^{-2}$, $|h_3''| = 1.97 \times 10^{-2}$, $|h_4| = 4.42$, $|h_4'| = 5.07$, $|h_4''| = 2.87$, $|h_5| = 6.6$, $|h_5'| = 2.67$, $|h_5''| = 1.86 \times 10^{-1}$, $|h_6| = |h_7| = |h_8| = 1000$, $\theta_\mu = 4.7 \times 10^{-3}$, $\xi_1 = 2 \times 10^{-2}$, $\xi_2 = 2 \times 10^{-3}$, $\alpha_{A_0^u} = 2 \times 10^{-2}$, $\alpha_{A_0^d} = 3.0$, $\chi_3 = 2 \times 10^{-2}$, $\chi_3' = 1 \times 10^{-3}$, $\chi_3'' = 4 \times 10^{-3}$, $\chi_4 = 7 \times 10^{-3}$, $\chi_4' = \chi_4'' = 1 \times 10^{-3}$, $\chi_5 = 9 \times 10^{-3}$, $\chi_5' = 5 \times 10^{-3}$, $\chi_5'' = 2 \times 10^{-3}$, $\chi_6 = \chi_7 = \chi_8 = 5 \times 10^{-3}$. All masses are in GeV, and phases are in rad.

and the fourth-generation quarks. An analysis of the dependence of the CEDM on χ_6 is exhibited in Fig. 10. Aside from h_6, other mass parameters that arise because of the new sector are h_7 and h_8. The dependence of the CEDM on $|h_8|$ is also exhibited in Fig. 10. Quite remarkably the CEDM is sensitive to both the mass scale and the phase that enters in the new sector.

Finally it is of interest to look at the total electric dipole moment obtained by adding the electric and the chromo-electric dipole moments. Figure 11 shows the variation of the EDM, the CEDM and the total EDM against the gluino phase, ξ_3. The analysis of Fig. 11 shows that, while the EDM may dominate the CEDM for some values of ξ_3, the opposite may happen for a different range of ξ_3. The analysis also suggests constructive interference between EDM and CEDM in some parts of the parameter space while there is destructive interferences in other parts (i.e., for $0 < \xi_3 < \pi$) leading to the cancellations mechanism [26,27].

VI. CONCLUSION

In this work we have given an analysis of the chromo-electric dipole moment of quarks and of the neutron arising in an extension of the MSSM where there is an additional vectorlike generation of quarks in the matter sector. Such an

extension brings in new sources of CP violation which can contribute to the chromoelectric dipole moment of quarks. The work presented here consists of analytical results on five different types of contributions to the chromoelectric dipole moments of quarks which include both nonsupersymmetric as well as supersymmetric loop contributions. In the nonsupersymmetric sector, we have contributions arising from the exchanges of the W and Z bosons in the loops, while in the supersymmetric sector, we have exchanges involving charginos, neutralinos and the gluino in the loop. We have also carried out a detailed numerical analysis of their relative contributions. Specifically it is found that there exists strong interference effects between the MSSM sector and the vectorlike quark sector which can drastically change both the sign and the magnitude of the quark EDMs. We have also investigated the possibility that the neutron EDM can be used as probe of the TeV scale physics. These results are of import as future experiment can improve the current limits up to 2 orders of magnitude, and thus the quark EDMs provide an important window to new physics beyond the standard model.

ACKNOWLEDGMENTS

P. N.'s research is supported in part by the NSF Grant No. PHY-1314774.

APPENDIX A: SQUARK MASS MATRICES

In this Appendix we give further details of the model discussed in Sec. II. As discussed in Sec. II, we allow for mixing between the vector generation and specifically the mirrors and the standard three generations of quarks. We also allow for mixing between the mirror generation and the fourth sequential generation assuming R parity conservation (for a recent review of R parity, see Ref. [37]). The superpotential allowing such mixings is given by

$$\begin{aligned} W = {} & \epsilon_{ij}[y_1\hat{H}_1^i\hat{q}_{1L}^j\hat{b}_{1L}^c + y_1'\hat{H}_2^j\hat{q}_{1L}^i\hat{t}_{1L}^c + y_2\hat{H}_1^i\hat{Q}^{cj}\hat{T}_L + y_2'\hat{H}_2^j\hat{Q}^{ci}\hat{B}_L \\ & + y_3\hat{H}_1^i\hat{q}_{2L}^j\hat{b}_{2L}^c + y_3'\hat{H}_2^j\hat{q}_{2L}^i\hat{t}_{2L}^c + y_4\hat{H}_1^i\hat{q}_{3L}^j\hat{b}_{3L}^c + y_4'\hat{H}_2^j\hat{q}_{3L}^i\hat{t}_{3L}^c + y_5\hat{H}_1^i\hat{q}_{4L}^j\hat{b}_{4L}^c + y_5'\hat{H}_2^j\hat{q}_{4L}^i\hat{t}_{4L}^c] \\ & + h_3\epsilon_{ij}\hat{Q}^{ci}\hat{q}_{1L}^j + h_3'\epsilon_{ij}\hat{Q}^{ci}\hat{q}_{2L}^j + h_3''\epsilon_{ij}\hat{Q}^{ci}\hat{q}_{3L}^j + h_4\hat{b}_{1L}^c\hat{B}_L + h_5\hat{t}_{1L}^c\hat{T}_L + h_4'\hat{b}_{2L}^c\hat{B}_L \\ & + h_5'\hat{t}_{2L}^c\hat{T}_L + h_4''\hat{b}_{3L}^c\hat{B}_L + h_5''\hat{t}_{3L}^c\hat{T}_L + h_6\epsilon_{ij}Q^iq_{4L}^j + h_7\hat{b}_{4L}^c\hat{B}_L + h_8\hat{t}_{4L}^c\hat{T}_L - \mu\epsilon_{ij}\hat{H}_1^i\hat{H}_2^j. \end{aligned} \tag{A1}$$

Here the couplings are in general complex. Thus, for example, μ is the complex Higgs mixing parameter so that $\mu = |\mu|e^{i\theta_\mu}$. The mass terms for the ups, mirror ups, downs and mirror downs arise from the term

$$\mathcal{L} = -\frac{1}{2}\frac{\partial^2 W}{\partial A_i \partial A_j}\psi_i\psi_j + \text{H.c.}, \tag{A2}$$

where ψ and A stand for generic two-component fermion and scalar fields. After spontaneous breaking of the electroweak symmetry, ($\langle H_1^1\rangle = v_1/\sqrt{2}$ and $\langle H_2^2\rangle = v_2/\sqrt{2}$), we have the following set of mass terms written in the four-component spinor notation so that

$$-\mathcal{L}_m = \bar{\xi}_R^T(M_u)\xi_L + \bar{\eta}_R^T(M_d)\eta_L + \text{H.c.}, \tag{A3}$$

where the basis vectors are defined in Eqs. (3) and (8).

Next we consider the mixing of the down squarks and the charged mirror sdowns. The mass squared matrix of the sdown-mirror sdown comes from three sources: the F term, the D term of the potential and the soft SUSY breaking terms. After spontaneous breaking of the electroweak symmetry the Lagrangian is given by

$$\mathcal{L} = \mathcal{L}_F + \mathcal{L}_D + \mathcal{L}_{\text{soft}}, \tag{A4}$$

where $\mathcal{L}_F$ is deduced from $F_i = \partial W/\partial A_i$, and $-\mathcal{L}_F = V_F = F_iF_i^*$ while the $\mathcal{L}_D$ is given by

$$\begin{aligned} -\mathcal{L}_D = {} & \frac{1}{2}m_Z^2\cos^2\theta_W\cos 2\beta\{\tilde{t}_L\tilde{t}_L^* - \tilde{b}_L\tilde{b}_L^* + \tilde{c}_L\tilde{c}_L^* - \tilde{s}_L\tilde{s}_L^* + \tilde{u}_L\tilde{u}_L^* - \tilde{d}_L\tilde{d}_L^* + \tilde{t}_{4L}\tilde{t}_{4L}^* - \tilde{b}_{4L}\tilde{b}_{4L}^* + \tilde{B}_R\tilde{B}_R^* - \tilde{T}_R\tilde{T}_R^*\} \\ & + \frac{1}{2}m_Z^2\sin^2\theta_W\cos 2\beta\Big\{-\frac{1}{3}\tilde{t}_L\tilde{t}_L^* + \frac{4}{3}\tilde{t}_R\tilde{t}_R^* - \frac{1}{3}\tilde{c}_L\tilde{c}_L^* + \frac{4}{3}\tilde{c}_R\tilde{c}_R^* - \frac{1}{3}\tilde{u}_L\tilde{u}_L^* + \frac{4}{3}\tilde{u}_R\tilde{u}_R^* + \frac{1}{3}\tilde{T}_R\tilde{T}_R^* - \frac{4}{3}\tilde{T}_L\tilde{T}_L^* - \frac{1}{3}\tilde{b}_L\tilde{b}_L^* \\ & - \frac{2}{3}\tilde{b}_R\tilde{b}_R^* - \frac{1}{3}\tilde{s}_L\tilde{s}_L^* - \frac{2}{3}\tilde{s}_R\tilde{s}_R^* - \frac{1}{3}\tilde{d}_L\tilde{d}_L^* - \frac{2}{3}\tilde{d}_R\tilde{d}_R^* + \frac{1}{3}\tilde{B}_R\tilde{B}_R^* \\ & + \frac{2}{3}\tilde{B}_L\tilde{B}_L^* - \frac{1}{3}\tilde{t}_{4L}\tilde{t}_{4L}^* + \frac{4}{3}\tilde{t}_{4R}\tilde{t}_{4R}^* - \frac{1}{3}\tilde{b}_{4L}\tilde{b}_{4L}^* - \frac{2}{3}\tilde{b}_{4R}\tilde{b}_{4R}^*\Big\}. \end{aligned} \tag{A5}$$

For $\mathcal{L}_{\rm soft}$ we assume the following form:

$$\begin{aligned}-\mathcal{L}_{\rm soft} &= M^2_{\tilde{1}L}\tilde{q}^{k*}_{1L}\tilde{q}^{k}_{1L} + M^2_{\tilde{4}L}\tilde{q}^{k*}_{4L}\tilde{q}^{k}_{4L} + M^2_{\tilde{2}L}\tilde{q}^{k*}_{2L}\tilde{q}^{k}_{2L} + M^2_{\tilde{3}L}\tilde{q}^{k*}_{3L}\tilde{q}^{k}_{3L} + M^2_{\tilde{Q}}\tilde{Q}^{ck*}\tilde{Q}^{ck} + M^2_{\tilde{t}_1}\tilde{t}^{c*}_{1L}\tilde{t}^{c}_{1L} \\ &+ M^2_{\tilde{b}_1}\tilde{b}^{c*}_{1L}\tilde{b}^{c}_{1L} + M^2_{\tilde{t}_2}\tilde{t}^{c*}_{2L}\tilde{t}^{c}_{2L} + M^2_{\tilde{b}_4}\tilde{b}^{c*}_{4L}\tilde{b}^{c}_{4L} + M^2_{\tilde{t}_4}\tilde{t}^{c*}_{4L}\tilde{t}^{c}_{4L} \\ &+ M^2_{\tilde{t}_3}\tilde{t}^{c*}_{3L}\tilde{t}^{c}_{3L} + M^2_{\tilde{b}_2}\tilde{b}^{c*}_{2L}\tilde{b}^{c}_{2L} + M^2_{\tilde{b}_3}\tilde{b}^{c*}_{3L}\tilde{b}^{c}_{3L} + M^2_{\tilde{B}}\tilde{B}^{*}_{L}\tilde{B}_{L} + M^2_{\tilde{T}}\tilde{T}^{*}_{L}\tilde{T}_{L} \\ &+ \epsilon_{ij}\{y_1 A_b H^i_1 \tilde{q}^j_{1L}\tilde{b}^c_{1L} - y'_1 A_t H^i_2 \tilde{q}^j_{1L}\tilde{t}^c_{1L} + y_5 A_{4b} H^i_1 \tilde{q}^j_{4L}\tilde{b}^c_{4L} - y'_5 A_{4t} H^i_2 \tilde{q}^j_{4L}\tilde{t}^c_{4L} + y_3 A_s H^i_1 \tilde{q}^j_{2L}\tilde{b}^c_{2L} \\ &- y'_3 A_c H^i_2 \tilde{q}^j_{2L}\tilde{t}^c_{2L} + y_4 A_d H^i_1 \tilde{q}^j_{3L}\tilde{b}^c_{3L} - y'_4 A_u H^i_2 \tilde{q}^j_{3L}\tilde{t}^c_{3L} + y_2 A_T H^i_1 \tilde{Q}^{cj}\tilde{T}_L - y'_2 A_B H^i_2 \tilde{Q}^{cj}\tilde{B}_L + \text{H.c.}\}. \end{aligned} \tag{A6}$$

Here $M_{\tilde{1}L}, M_{\tilde{T}}$, etc., are the soft masses, and A_t, A_b, etc., are the trilinear couplings. The trilinear couplings are complex, and we define their phases so that

$$A_b = |A_b|e^{i\alpha_{A_b}}, \qquad A_t = |A_t|e^{i\alpha_{A_t}}, \ldots. \tag{A7}$$

From these terms we construct the scalar mass squared matrices. Thus, we define the scalar mass squared matrix $M^2_{\tilde{d}}$ in the basis $(\tilde{b}_L, \tilde{B}_L, \tilde{b}_R, \tilde{B}_R, \tilde{s}_L, \tilde{s}_R, \tilde{d}_L, \tilde{d}_R, \tilde{b}_{4L}, \tilde{b}_{4R})$. We label the matrix elements of these as $(M^2_{\tilde{d}})_{ij} = M^2_{ij}$ which is a Hermitian matrix. We can diagonalize this Hermitian mass squared matrix by the unitary transformation

$$\tilde{D}^{d\dagger} M^2_{\tilde{d}} \tilde{D}^d = \text{diag}(M^2_{\tilde{d}_1}, M^2_{\tilde{d}_2}, M^2_{\tilde{d}_3}, M^2_{\tilde{d}_4}, M^2_{\tilde{d}_5}, M^2_{\tilde{d}_6}, M^2_{\tilde{d}_7}, M^2_{\tilde{d}_8} M^2_{\tilde{d}_9}, M^2_{\tilde{d}_{10}}). \tag{A8}$$

Similarly we write the mass squared matrix in the up-squark sector in the basis $(\tilde{t}_L, \tilde{T}_L, \tilde{t}_R, \tilde{T}_R, \tilde{c}_L, \tilde{c}_R, \tilde{u}_L, \tilde{u}_R, \tilde{t}_{4L}, \tilde{t}_{4R})$. Thus, here we denote the up-squark mass squared matrix in the form $(M^2_{\tilde{u}})_{ij} = m^2_{ij}$ which is also a Hermitian matrix. We can diagonalize this mass square matrix by the unitary transformation

$$\tilde{D}^{u\dagger} M^2_{\tilde{u}} \tilde{D}^u = \text{diag}(M^2_{\tilde{u}_1}, M^2_{\tilde{u}_2}, M^2_{\tilde{u}_3}, M^2_{\tilde{u}_4}, M^2_{\tilde{u}_5}, M^2_{\tilde{u}_6}, M^2_{\tilde{u}_7}, M^2_{\tilde{u}_8}, M^2_{\tilde{u}_9}, M^2_{\tilde{u}_{10}}). \tag{A9}$$

APPENDIX B: W, Z, $\tilde{\chi}^{\pm}$, $\tilde{\chi}^0$, $\tilde{g}$ COUPLINGS WITH QUARKS

1. W-quark-quark couplings

The couplings that enter in the W-quark-squark interactions of Eq. (13) are defined so that

$$\begin{aligned}G^W_{L_{ji}} &= \frac{g}{\sqrt{2}}[D^{u*}_{L5j}D^d_{L5i} + D^{u*}_{L4j}D^d_{L4i} + D^{u*}_{L3j}D^d_{L3i} \\ &+ D^{u*}_{L1j}D^d_{L1i}],\end{aligned} \tag{B1}$$

$$G^W_{R_{ji}} = \frac{g}{\sqrt{2}}[D^{u*}_{R2j}D^d_{R2i}]. \tag{B2}$$

2. Z-quark-quark couplings

The couplings that enter in the Z-up-quark interactions of Eq. (18) are defined so that

$$\begin{aligned}C^{uZ}_{L_{ji}} &= \frac{g}{\cos\theta_W}[x_1(D^{u*}_{L5j}D^u_{L5i} + D^{u*}_{L4j}D^u_{L4i} + D^{u*}_{L1j}D^u_{L1i} \\ &+ D^{u*}_{L3j}D^u_{L3i}) + y_1 D^{u*}_{L2j}D^u_{L2i}],\end{aligned} \tag{B3}$$

and

$$\begin{aligned}C^{uZ}_{R_{ji}} &= \frac{g}{\cos\theta_W}[y_1(D^{u*}_{R5j}D^u_{R5i} + D^{u*}_{R4j}D^u_{R4i} + D^{u*}_{R1j}D^u_{R1i} \\ &+ D^{u*}_{R3j}D^u_{R3i}) + x_1 D^{u*}_{R2j}D^u_{R2i}],\end{aligned} \tag{B4}$$

where

$$x_1 = \frac{1}{2} - \frac{2}{3}\sin^2\theta_W, \qquad y_1 = -\frac{2}{3}\sin^2\theta_W. \tag{B5}$$

The couplings that enter in the Z-down-quark interactions of Eq. (20) are defined so that

$$\begin{aligned}C^{dZ}_{L_{ji}} &= \frac{g}{\cos\theta_W}[x_2(D^{d*}_{L5j}D^d_{L5i} + D^{d*}_{L4j}D^d_{L4i} + D^{d*}_{L1j}D^d_{L1i} \\ &+ D^{d*}_{L3j}D^d_{L3i}) + y_2 D^{d*}_{L2j}D^d_{L2i}],\end{aligned} \tag{B6}$$

and

$$\begin{aligned}C^{dZ}_{R_{ji}} &= \frac{g}{\cos\theta_W}[y_2(D^{d*}_{R5j}D^d_{R5i} + D^{d*}_{R4j}D^d_{R4i} + D^{d*}_{R1j}D^d_{R1i} \\ &+ D^{d*}_{R3j}D^d_{R3i}) + x_2 D^{d*}_{R2j}D^d_{R2i}],\end{aligned} \tag{B7}$$

where

$$x_2 = -\frac{1}{2} + \frac{1}{3}\sin^2\theta_W, \qquad y_2 = \frac{1}{3}\sin^2\theta_W. \tag{B8}$$

3. Chargino-quark-squark couplings

The couplings that enter in the chargino-up-quark-down-squark interactions of Eq. (23) are given by

$$\begin{aligned} C^{Lu}_{jik} = g(&-\kappa_u V^*_{i2} D^{u*}_{R4j} \tilde{D}^d_{7k} - \kappa_c V^*_{i2} D^{u*}_{R3j} \tilde{D}^d_{5k} - \kappa_t V^*_{i2} D^{u*}_{R1j} \tilde{D}^d_{1k} \\ &- \kappa_{4t} V^*_{i2} D^{u*}_{R5j} \tilde{D}^d_{9k} - \kappa_B V^*_{i2} D^{u*}_{R2j} \tilde{D}^d_{2k} + V^*_{i1} D^{u*}_{R2j} \tilde{D}^d_{4k}), \end{aligned} \tag{B9}$$

$$\begin{aligned} C^{Ru}_{jik} = g(&-\kappa_d U_{i2} D^{u*}_{L4j} \tilde{D}^d_{8k} - \kappa_s U_{i2} D^{u*}_{L3j} \tilde{D}^d_{6k} - \kappa_b U_{i2} D^{u*}_{L1j} \tilde{D}^d_{3k} \\ &- \kappa_{4b} U_{i2} D^{u*}_{L5j} \tilde{D}^d_{10k} - \kappa_T U_{i2} D^{u*}_{L2j} \tilde{D}^d_{4k} \\ &+ U_{i1} D^{u*}_{L4j} \tilde{D}^d_{7k} + U_{i1} D^{u*}_{L3j} \tilde{D}^d_{5k} + U_{i1} D^{u*}_{L1j} \tilde{D}^d_{1k} + U_{i1} D^{u*}_{L5j} \tilde{D}^d_{9k}). \end{aligned} \tag{B10}$$

The couplings that enter in the chargino-down-quark-up-squark interactions of Eq. (22) are given by

$$\begin{aligned} C^{Ld}_{jik} = g(&-\kappa_d U^*_{i2} D^{d*}_{R4j} \tilde{D}^u_{7k} - \kappa_s U^*_{i2} D^{d*}_{R3j} \tilde{D}^u_{5k} \\ &- \kappa_b U^*_{i2} D^{d*}_{R1j} \tilde{D}^u_{1k} - \kappa_{4b} U^*_{i2} D^{d*}_{R5j} \tilde{D}^u_{9k} - \kappa_T U^*_{i2} D^{d*}_{R2j} \tilde{D}^u_{2k} + U^*_{i1} D^{d*}_{R2j} \tilde{D}^u_{4k}), \end{aligned} \tag{B11}$$

$$\begin{aligned} C^{Rd}_{jik} = g(&-\kappa_u V_{i2} D^{d*}_{L4j} \tilde{D}^u_{8k} - \kappa_c V_{i2} D^{d*}_{L3j} \tilde{D}^u_{6k} - \kappa_t V_{i2} D^{d*}_{L1j} \tilde{D}^u_{3k} - \kappa_{4t} V_{i2} D^{d*}_{L5j} \tilde{D}^u_{10k} \\ &- \kappa_B V_{i2} D^{d*}_{L2j} \tilde{D}^u_{4k} + V_{i1} D^{d*}_{L4j} \tilde{D}^u_{7k} + V_{i1} D^{d*}_{L3j} \tilde{D}^u_{5k} + V_{i1} D^{d*}_{L1j} \tilde{D}^u_{1k} + V_{i1} D^{d*}_{L5j} \tilde{D}^u_{9k}), \end{aligned} \tag{B12}$$

where

$$(\kappa_T, \kappa_b, \kappa_s, \kappa_d, \kappa_{4b}) = \frac{(m_T, m_b, m_s, m_d, m_{4b})}{\sqrt{2} m_W \cos\beta}, \tag{B13}$$

$$(\kappa_B, \kappa_t, \kappa_c, \kappa_u, \kappa_{4t}) = \frac{(m_B, m_t, m_c, m_u, m_{4t})}{\sqrt{2} m_W \sin\beta}. \tag{B14}$$

and

$$U^* M_C V = \mathrm{diag}(m_{\tilde{\chi}^-_1}, m_{\tilde{\chi}^-_2}). \tag{B15}$$

4. Neutralino-quark-squark couplings

We first give discuss the couplings that enter the interactions in the mass diagonal basis involving the up quarks, up squarks and neutralinos of Eq. (28). Here we have

$$\begin{aligned} C'^L_{uijk} = \sqrt{2}(&\alpha_{uj} D^{u*}_{R4i} \tilde{D}^u_{7k} - \gamma_{uj} D^{u*}_{R4i} \tilde{D}^u_{8k} + \alpha_{cj} D^{u*}_{R3i} \tilde{D}^u_{5k} - \gamma_{cj} D^{u*}_{R3i} \tilde{D}^u_{6k} + \alpha_{tj} D^{u*}_{R1i} \tilde{D}^u_{1k} \\ &- \gamma_{tj} D^{u*}_{R1i} \tilde{D}^u_{3k} + \alpha_{4tj} D^{u*}_{R5i} \tilde{D}^u_{9k} - \gamma_{4tj} D^{u*}_{R5i} \tilde{D}^u_{10k} + \beta_{Tj} D^{u*}_{R2i} \tilde{D}^u_{4k} - \delta_{Tj} D^{u*}_{R2i} \tilde{D}^u_{2k}), \end{aligned} \tag{B16}$$

$$\begin{aligned} C'^R_{uijk} = \sqrt{2}(&\beta_{uj} D^{u*}_{L4i} \tilde{D}^u_{7k} - \delta_{uj} D^{u*}_{L4i} \tilde{D}^u_{8k} + \beta_{cj} D^{u*}_{L3i} \tilde{D}^u_{5k} - \delta_{cj} D^{u*}_{L3i} \tilde{D}^u_{6k} + \beta_{tj} D^{u*}_{L1i} \tilde{D}^u_{1k} \\ &- \delta_{tj} D^{u*}_{L1i} \tilde{D}^u_{3k} + \beta_{4tj} D^{u*}_{L5i} \tilde{D}^u_{9k} - \delta_{4tj} D^{u*}_{L5i} \tilde{D}^u_{10k} + \alpha_{Tj} D^{u*}_{L2i} \tilde{D}^u_{4k} - \gamma_{Tj} D^{u*}_{L2i} \tilde{D}^u_{2k}), \end{aligned} \tag{B17}$$

where

$$\alpha_{Tj} = \frac{g m_T X^*_{3j}}{2 m_W \cos\beta}; \qquad \beta_{Tj} = -\frac{2}{3} e X'_{1j} + \frac{g}{\cos\theta_W} X'_{2j} \left(-\frac{1}{2} + \frac{2}{3}\sin^2\theta_W \right) \tag{B18}$$

$$\gamma_{Tj} = -\frac{2}{3} e X'^{*}_{1j} + \frac{2}{3}\frac{g \sin^2\theta_W}{\cos\theta_W} X'^{*}_{2j}; \qquad \delta_{Tj} = -\frac{g m_T X_{3j}}{2 m_W \cos\beta} \tag{B19}$$

and

$$\alpha_{4tj} = \frac{g m_{4t} X_{4j}}{2 m_W \sin\beta}; \qquad \alpha_{tj} = \frac{g m_t X_{4j}}{2 m_W \sin\beta}; \qquad \alpha_{cj} = \frac{g m_c X_{4j}}{2 m_W \sin\beta}; \qquad \alpha_{uj} = \frac{g m_u X_{4j}}{2 m_W \sin\beta} \tag{B20}$$

$$\delta_{4tj} = -\frac{g m_{4t} X^{*}_{4j}}{2 m_W \sin\beta}; \qquad \delta_{tj} = -\frac{g m_t X^{*}_{4j}}{2 m_W \sin\beta}; \qquad \delta_{cj} = -\frac{g m_c X^{*}_{4j}}{2 m_W \sin\beta}; \qquad \delta_{uj} = -\frac{g m_u X^{*}_{4j}}{2 m_W \sin\beta} \tag{B21}$$

and where

$$\beta_{4tj} = \beta_{tj} = \beta_{cj} = \beta_{uj} = \frac{2}{3} e X'^{*}_{1j} + \frac{g}{\cos\theta_W} X'^{*}_{2j}\left(\frac{1}{2} - \frac{2}{3}\sin^2\theta_W\right) \tag{B22}$$

$$\gamma_{4tj} = \gamma_{tj} = \gamma_{cj} = \gamma_{uj} = \frac{2}{3} e X'_{1j} - \frac{2}{3}\frac{g \sin^2\theta_W}{\cos\theta_W} X'_{2j}. \tag{B23}$$

Similarly for the couplings that enter the interactions in the mass diagonal basis involving the down quarks, down squarks and neutralinos of Eq. (29), we have

$$\begin{aligned} C'^{L}_{dijk} = \sqrt{2}(&\alpha_{dj} D^{d*}_{R4i} \tilde{D}^{d}_{7k} - \gamma_{dj} D^{d*}_{R4i} \tilde{D}^{d}_{8k} + \alpha_{sj} D^{d*}_{R3i} \tilde{D}^{d}_{5k} - \gamma_{sj} D^{d*}_{R3i} \tilde{D}^{d}_{6k} + \alpha_{bj} D^{d*}_{R1i} \tilde{D}^{d}_{1k} - \gamma_{bj} D^{d*}_{R1i} \tilde{D}^{d}_{3k} \\ &+ \alpha_{4bj} D^{d*}_{R5i} \tilde{D}^{d}_{9k} - \gamma_{4bj} D^{d*}_{R5i} \tilde{D}^{d}_{10k} + \beta_{Bj} D^{d*}_{R2i} \tilde{D}^{d}_{4k} - \delta_{Bj} D^{d*}_{R2i} \tilde{D}^{d}_{2k}), \end{aligned} \tag{B24}$$

and

$$\begin{aligned} C'^{R}_{dijk} = \sqrt{2}(&\beta_{dj} D^{d*}_{L4i} \tilde{D}^{d}_{7k} - \delta_{dj} D^{d*}_{L4i} \tilde{D}^{d}_{8k} + \beta_{sj} D^{d*}_{L3i} \tilde{D}^{d}_{5k} - \delta_{sj} D^{d*}_{L3i} \tilde{D}^{d}_{6k} + \beta_{bj} D^{d*}_{L1i} \tilde{D}^{d}_{1k} - \delta_{bj} D^{d*}_{L1i} \tilde{D}^{d}_{3k} \\ &+ \beta_{4bj} D^{d*}_{L5i} \tilde{D}^{d}_{9k} - \delta_{4bj} D^{d*}_{L5i} \tilde{D}^{d}_{10k} + \alpha_{Bj} D^{d*}_{L2i} \tilde{D}^{d}_{4k} - \gamma_{Bj} D^{d*}_{L2i} \tilde{D}^{d}_{2k}), \end{aligned} \tag{B25}$$

where

$$\alpha_{Bj} = \frac{g m_B X^{*}_{4j}}{2 m_W \sin\beta}; \qquad \beta_{Bj} = \frac{1}{3} e X'_{1j} + \frac{g}{\cos\theta_W} X'_{2j}\left(\frac{1}{2} - \frac{1}{3}\sin^2\theta_W\right) \tag{B26}$$

$$\gamma_{Bj} = \frac{1}{3} e X'^{*}_{1j} - \frac{1}{3}\frac{g \sin^2\theta_W}{\cos\theta_W} X'^{*}_{2j}; \qquad \delta_{Bj} = -\frac{g m_B X_{4j}}{2 m_W \sin\beta} \tag{B27}$$

and

$$\alpha_{4bj} = \frac{g m_{4b} X_{3j}}{2 m_W \cos\beta}; \qquad \alpha_{bj} = \frac{g m_b X_{3j}}{2 m_W \cos\beta}; \qquad \alpha_{sj} = \frac{g m_s X_{3j}}{2 m_W \cos\beta}; \qquad \alpha_{dj} = \frac{g m_d X_{3j}}{2 m_W \cos\beta} \tag{B28}$$

$$\delta_{4bj} = -\frac{g m_{4b} X^{*}_{3j}}{2 m_W \cos\beta}; \qquad \delta_{bj} = -\frac{g m_b X^{*}_{3j}}{2 m_W \cos\beta}; \qquad \delta_{sj} = -\frac{g m_s X^{*}_{3j}}{2 m_W \cos\beta}; \qquad \delta_{dj} = -\frac{g m_d X^{*}_{3j}}{2 m_W \cos\beta} \tag{B29}$$

and where

$$\beta_{4bj} = \beta_{bj} = \beta_{sj} = \beta_{dj} = -\frac{1}{3} e X'^{*}_{1j} + \frac{g}{\cos\theta_W} X'^{*}_{2j}\left(-\frac{1}{2} + \frac{1}{3}\sin^2\theta_W\right) \tag{B30}$$

$$\gamma_{4bj} = \gamma_{bj} = \gamma_{sj} = \gamma_{dj} = -\frac{1}{3} e X'_{1j} + \frac{1}{3}\frac{g \sin^2\theta_W}{\cos\theta_W} X'_{2j} \tag{B31}$$

Here X' are defined by

$$X'_{1i} = X_{1i}\cos\theta_W + X_{2i}\sin\theta_W \tag{B32}$$

$$X'_{2i} = -X_{1i}\sin\theta_W + X_{2i}\cos\theta_W, \tag{B33}$$

where X diagonalizes the neutralino mass matrix and is defined by

$$X^T M_{\chi^0} X = \mathrm{diag}(m_{\tilde{\chi}^0_1}, m_{\tilde{\chi}^0_2}, m_{\tilde{\chi}^0_3}, m_{\tilde{\chi}^0_4}). \tag{B34}$$

5. Gluino-quark-squark-couplings

The couplings that enter in the gluino-quark-squark interactions of Eq. (32) are given by

$$C_{L_{lm}} = (D^{q*}_{R2l}\tilde{D}^q_{4m} - D^{q*}_{R5l}\tilde{D}^q_{10m} - D^{q*}_{R4l}\tilde{D}^q_{8m} - D^{q*}_{R3l}\tilde{D}^q_{6m} - D^{q*}_{R1l}\tilde{D}^q_{3m})e^{-i\xi_3/2}, \tag{B35}$$

and

$$C_{R_{lm}} = (D^{q*}_{L4l}\tilde{D}^q_{7m} + D^{q*}_{L5l}\tilde{D}^q_{9m} + D^{q*}_{L3l}\tilde{D}^q_{5m} + D^{q*}_{L1l}\tilde{D}^q_{1m} - D^{q*}_{L2l}\tilde{D}^q_{2m})e^{i\xi_3/2}, \tag{B36}$$

where ξ_3 is the phase of the gluino mass.

APPENDIX C: MASS SQUARED MATRICES FOR THE SCALARS

We define the scalar mass squared matrix $M^2_{\tilde{d}}$ in the basis $(\tilde{b}_L, \tilde{B}_L, \tilde{b}_R, \tilde{B}_R, \tilde{s}_L, \tilde{s}_R, \tilde{d}_L, \tilde{d}_R, \tilde{b}_{4L}, \tilde{b}_{4R})$. We label the matrix elements of these as $(M^2_{\tilde{d}})_{ij} = M^2_{ij}$ where the elements of the matrix are given by

$$\begin{aligned}
M^2_{11} &= M^2_{\tilde{1}L} + \frac{v_1^2|y_1|^2}{2} + |h_3|^2 - m_Z^2\cos 2\beta\left(\frac{1}{2} - \frac{1}{3}\sin^2\theta_W\right),\\
M^2_{22} &= M^2_{\tilde{B}} + \frac{v_2^2|y'_2|^2}{2} + |h_4|^2 + |h'_4|^2 + |h''_4|^2 + |h_7|^2 + \frac{1}{3}m_Z^2\cos 2\beta\sin^2\theta_W,\\
M^2_{33} &= M^2_{\tilde{b}_1} + \frac{v_1^2|y_1|^2}{2} + |h_4|^2 - \frac{1}{3}m_Z^2\cos 2\beta\sin^2\theta_W,\\
M^2_{44} &= M^2_{\tilde{Q}} + \frac{v_2^2|y'_2|^2}{2} + |h_3|^2 + |h'_3|^2 + |h''_3|^2 + |h_6|^2 + m_Z^2\cos 2\beta\left(\frac{1}{2} - \frac{1}{3}\sin^2\theta_W\right),\\
M^2_{55} &= M^2_{\tilde{2}L} + \frac{v_1^2|y_3|^2}{2} + |h'_3|^2 - m_Z^2\cos 2\beta\left(\frac{1}{2} - \frac{1}{3}\sin^2\theta_W\right),\\
M^2_{66} &= M^2_{\tilde{b}_2} + \frac{v_1^2|y_3|^2}{2} + |h'_4|^2 - \frac{1}{3}m_Z^2\cos 2\beta\sin^2\theta_W,\\
M^2_{77} &= M^2_{\tilde{3}L} + \frac{v_1^2|y_4|^2}{2} + |h''_3|^2 - m_Z^2\cos 2\beta\left(\frac{1}{2} - \frac{1}{3}\sin^2\theta_W\right),\\
M^2_{88} &= M^2_{\tilde{b}_3} + \frac{v_1^2|y_4|^2}{2} + |h''_4|^2 - \frac{1}{3}m_Z^2\cos 2\beta\sin^2\theta_W.\\
M^2_{99} &= M^2_{\tilde{4}L} + \frac{v_1^2|y_5|^2}{2} + |h_6|^2 - m_Z^2\cos 2\beta\left(\frac{1}{2} - \frac{1}{3}\sin^2\theta_W\right)\\
M^2_{1010} &= M^2_{\tilde{b}_4} + \frac{v_1^2|y_5|^2}{2} + |h_7|^2 - \frac{1}{3}m_Z^2\cos 2\beta\sin^2\theta_W.
\end{aligned} \tag{C1}$$

$$M^2_{12}=M^{2*}_{21}=\frac{v_2 y'_2 h^*_3}{\sqrt{2}}+\frac{v_1 h_4 y^*_1}{\sqrt{2}},\qquad M^2_{13}=M^{2*}_{31}=\frac{y^*_1}{\sqrt{2}}(v_1 A^*_b-\mu v_2),\qquad M^2_{14}=M^{2*}_{41}=0,$$

$$M^2_{15}=M^{2*}_{51}=h'_3 h^*_3,\qquad M^2_{16}=M^{2*}_{61}=0,\qquad M^2_{17}=M^{2*}_{71}=h''_3 h^*_3,\qquad M^{2*}_{18}=M^{2*}_{81}=0,\qquad M^2_{19}=M^{2*}_{91}=h^*_3 h_6,$$

$$M^2_{110}=M^{2*}_{101}=0,\qquad M^2_{23}=M^{2*}_{32}=0,\qquad M^2_{24}=M^{2*}_{42}=\frac{y'^*_2}{\sqrt{2}}(v_2 A^*_B-\mu v_1),\qquad M^2_{25}=M^{2*}_{52}=\frac{v_2 h'_3 y'^*_2}{\sqrt{2}}+\frac{v_1 y_3 h^*_4}{\sqrt{2}},$$

$$M^2_{26}=M^{2*}_{62}=0,\qquad M^2_{27}=M^{2*}_{72}=\frac{v_2 h''_3 y'^*_2}{\sqrt{2}}+\frac{v_1 y_4 h''^*_4}{\sqrt{2}},\qquad M^2_{28}=M^{2*}_{82}=0,$$

$$M^2_{29}=M^{2*}_{92}=\frac{v_1 h^*_7 y_5}{\sqrt{2}}+\frac{v_2 y'^*_2 h_6}{\sqrt{2}},\qquad M^2_{210}=M^{2*}_{102}=0,$$

$$M^2_{34}=M^{2*}_{43}=\frac{v_2 h_4 y'^*_2}{\sqrt{2}}+\frac{v_1 y_1 h^*_3}{\sqrt{2}},\qquad M^2_{35}=M^{2*}_{53}=0,\qquad M^2_{36}=M^{2*}_{63}=h_4 h'^*_4,$$

$$M^2_{37}=M^{2*}_{73}=0,\qquad M^2_{38}=M^{2*}_{83}=h_4 h''^*_4,$$

$$M^2_{39}=M^{2*}_{93}=0,\qquad M^2_{310}=M^{2*}_{103}=h_4 h^*_7,$$

$$M^2_{45}=M^{2*}_{54}=0,\qquad M^2_{46}=M^{2*}_{64}=\frac{v_2 y'_2 h'^*_4}{\sqrt{2}}+\frac{v_1 h'_3 y^*_3}{\sqrt{2}},$$

$$M^2_{47}=M^{2*}_{74}=0,\qquad M^2_{48}=M^{2*}_{84}=\frac{v_2 y'_2 h''^*_4}{\sqrt{2}}+\frac{v_1 h''_3 y^*_4}{\sqrt{2}},$$

$$M^2_{49}=M^{2*}_{94}=0,\qquad M^2_{410}=M^{2*}_{104}=\frac{v_2 y'_2 h^*_7}{\sqrt{2}}+\frac{v_1 h_6 y^*_5}{\sqrt{2}},$$

$$M^2_{56}=M^{2*}_{65}=\frac{y^*_3}{\sqrt{2}}(v_1 A^*_s-\mu v_2),\qquad M^2_{57}=M^{2*}_{75}=h''_3 h'^*_3,$$

$$M^2_{58}=M^{2*}_{85}=0,\qquad M^2_{59}=M^{2*}_{95}=h'^*_3 h_6,\qquad M^2_{510}=M^{2*}_{105}=0,\qquad M^2_{67}=M^{2*}_{76}=0,$$

$$M^2_{68}=M^{2*}_{86}=h'_4 h''^*_4,\qquad M^2_{69}=M^{2*}_{96}=0,\qquad M^2_{610}=M^{2*}_{106}=h'_4 h^*_7,\qquad M^2_{78}=M^{2*}_{87}=\frac{y^*_4}{\sqrt{2}}(v_1 A^*_d-\mu v_2).$$

$$M^2_{79}=M^{2*}_{97}=h''^*_3 h_6,\qquad M^2_{710}=M^{2*}_{107}=0$$

$$M^2_{89}=M^{2*}_{98}=0,\qquad M^2_{810}=M^{2*}_{108}=h''_4 h^*_7,\qquad M^2_{910}=M^{2*}_{109}=\frac{y^*_5}{\sqrt{2}}(v_1 A^*_{4b}-\mu v_2).$$

We can diagonalize this Hermitian mass squared matrix by the unitary transformation

$$\tilde{D}^{d\dagger} M^2_{\tilde{d}} \tilde{D}^d = \mathrm{diag}(M^2_{\tilde{d}_1}, M^2_{\tilde{d}_2}, M^2_{\tilde{d}_3}, M^2_{\tilde{d}_4}, M^2_{\tilde{d}_5}, M^2_{\tilde{d}_6}, M^2_{\tilde{d}_7}, M^2_{\tilde{d}_8}, M^2_{\tilde{d}_9}, M^2_{\tilde{d}_{10}}). \tag{C2}$$

Next we write the mass squared matrix in the sups sector the basis $(\tilde{t}_L, \tilde{T}_L, \tilde{t}_R, \tilde{T}_R, \tilde{c}_L, \tilde{c}_R, \tilde{u}_L, \tilde{u}_R, \tilde{t}_{4L}, \tilde{t}_{4R})$. Thus, here we denote the sups mass squared matrix in the form $(M^2_{\tilde{u}})_{ij} = m^2_{ij}$ where

$$
\begin{aligned}
m_{11}^2 &= M_{\tilde{1}L}^2 + \frac{v_2^2|y_1'|^2}{2} + |h_3|^2 + m_Z^2\cos 2\beta\left(\frac{1}{2} - \frac{2}{3}\sin^2\theta_W\right),\\
m_{22}^2 &= M_{\tilde{T}}^2 + \frac{v_1^2|y_2|^2}{2} + |h_5|^2 + |h_5'|^2 + |h_5''|^2 + |h_8|^2 - \frac{2}{3}m_Z^2\cos 2\beta\sin^2\theta_W,\\
m_{33}^2 &= M_{\tilde{t}_1}^2 + \frac{v_2^2|y_1'|^2}{2} + |h_5|^2 + \frac{2}{3}m_Z^2\cos 2\beta\sin^2\theta_W,\\
m_{44}^2 &= M_{\tilde{Q}}^2 + \frac{v_1^2|y_2|^2}{2} + |h_3|^2 + |h_3'|^2 + |h_3''|^2 + |h_6|^2 - m_Z^2\cos 2\beta\left(\frac{1}{2} - \frac{2}{3}\sin^2\theta_W\right),\\
m_{55}^2 &= M_{\tilde{2}L}^2 + \frac{v_2^2|y_3'|^2}{2} + |h_3'|^2 + m_Z^2\cos 2\beta\left(\frac{1}{2} - \frac{2}{3}\sin^2\theta_W\right),\\
m_{66}^2 &= M_{\tilde{t}_2}^2 + \frac{v_2^2|y_3'|^2}{2} + |h_5'|^2 + \frac{2}{3}m_Z^2\cos 2\beta\sin^2\theta_W,\\
m_{77}^2 &= M_{\tilde{3}L}^2 + \frac{v_2^2|y_4'|^2}{2} + |h_3''|^2 + m_Z^2\cos 2\beta\left(\frac{1}{2} - \frac{2}{3}\sin^2\theta_W\right),\\
m_{88}^2 &= M_{\tilde{t}_3}^2 + \frac{v_2^2|y_4'|^2}{2} + |h_5''|^2 + \frac{2}{3}m_Z^2\cos 2\beta\sin^2\theta_W,\\
m_{99}^2 &= M_{\tilde{4}L}^2 + \frac{v_2^2|y_5'|^2}{2} + |h_6|^2 + m_Z^2\cos 2\beta\left(\frac{1}{2} - \frac{2}{3}\sin^2\theta_W\right),\\
m_{1010}^2 &= M_{\tilde{t}_4}^2 + \frac{v_2^2|y_5'|^2}{2} + |h_8|^2 + \frac{2}{3}m_Z^2\cos 2\beta\sin^2\theta_W.
\end{aligned}
$$

$$
\begin{aligned}
&m_{12}^2 = m_{21}^{2*} = -\frac{v_1 y_2 h_3^*}{\sqrt{2}} + \frac{v_2 h_5 y_1'^*}{\sqrt{2}}, \qquad m_{13}^2 = m_{31}^{2*} = \frac{y_1'^*}{\sqrt{2}}(v_2 A_t^* - \mu v_1), \qquad m_{14}^2 = m_{41}^{2*} = 0,\\
&m_{15}^2 = m_{51}^{2*} = h_3' h_3^*, \qquad m_{16}^{2*} = m_{61}^{2*} = 0, \qquad m_{17}^{2*} = m_{71}^{2*} = h_3'' h_3^*, \qquad m_{18}^{2*} = m_{81}^{2*} = 0,\\
&m_{23}^2 = m_{32}^{2*} = 0, \qquad m_{24}^2 = m_{42}^{2*} = \frac{y_2^*}{\sqrt{2}}(v_1 A_T^* - \mu v_2), \qquad m_{25}^2 = m_{52}^{2*} = -\frac{v_1 h_3' y_2^*}{\sqrt{2}} + \frac{v_2 y_3' h_5'^*}{\sqrt{2}},\\
&m_{26}^2 = m_{62}^{2*} = 0, \qquad m_{27}^2 = m_{72}^{2*} = -\frac{v_1 h_3'' y_2^*}{\sqrt{2}} + \frac{v_2 y_4' h_5''^*}{\sqrt{2}}, \qquad m_{28}^2 = m_{82}^{2*} = 0,\\
&m_{34}^2 = m_{43}^{2*} = \frac{v_1 h_5 y_2^*}{\sqrt{2}} - \frac{v_2 y_1' h_3^*}{\sqrt{2}}, \qquad m_{35}^2 = m_{53}^{2*} = 0, \qquad m_{36}^2 = m_{63}^{2*} = h_5 h_5'^*,\\
&m_{37}^2 = m_{73}^{2*} = 0, \qquad m_{38}^2 = m_{83}^{2*} = h_5 h_5''^*,\\
&m_{45}^2 = m_{54}^{2*} = 0, \qquad m_{46}^2 = m_{64}^{2*} = -\frac{y_3'^* v_2 h_3'}{\sqrt{2}} + \frac{v_1 y_2 h_5'^*}{\sqrt{2}},\\
&m_{47}^2 = m_{74}^{2*} = 0, \qquad m_{48}^2 = m_{84}^{2*} = \frac{v_1 y_2 h_5''^*}{\sqrt{2}} - \frac{v_2 y_4'^* h_3''}{\sqrt{2}},\\
&m_{56}^2 = m_{65}^{2*} = \frac{y_3'^*}{\sqrt{2}}(v_2 A_c^* - \mu v_1),\\
&m_{57}^2 = m_{75}^{2*} = h_3'' h_3'^*, \qquad m_{58}^2 = m_{85}^{2*} = 0,\\
&m_{67}^2 = m_{76}^{2*} = 0, \qquad m_{68}^2 = m_{86}^{2*} = h_5' h_5''^*,\\
&m_{78}^2 = m_{87}^{2*} = \frac{y_4'^*}{\sqrt{2}}(v_2 A_u^* - \mu v_1),\\
&m_{19}^2 = m_{91}^{2*} = h_6 h_3^*, \qquad m_{110}^2 = m_{101}^{2*} = 0,
\end{aligned}
$$

$$
\begin{aligned}
&m^2_{29} = m^{2*}_{92} = -\frac{y_2^* v_1 h_6}{\sqrt{2}} + \frac{v_2 y_5^* h_8}{\sqrt{2}},\\
&m^2_{210} = m^{2*}_{102} = 0, \qquad m^2_{39} = m^{2*}_{93} = 0,\\
&m^2_{310} = m^{2*}_{103} = h_5 h_8^*,\\
&m^2_{49} = m^{2*}_{94} = 0, \qquad m^2_{410} = m^{2*}_{104} = -\frac{y_5'^* v_2 h_6}{\sqrt{2}} + \frac{v_1 y_2 h_8^*}{\sqrt{2}},\\
&m^2_{59} = m^{2*}_{95} = h_6 h_3'^*, \qquad m^2_{510} = m^{2*}_{105} = 0\\
&m^2_{69} = m^{2*}_{96} = 0, \qquad m^2_{610} = m^{2*}_{106} = h_5' h_8^*\\
&m^2_{79} = m^{2*}_{97} = h_6 h_3''^*, \qquad m^2_{710} = m^{2*}_{107} = 0,\\
&m^2_{89} = m^{2*}_{98} = 0, \qquad m^2_{810} = m^{2*}_{108} = h_5'' h_8^*,\\
&m^2_{910} = m^{2*}_{109} = \frac{y_5'^*}{\sqrt{2}}(v_2 A^*_{4t} - \mu v_1)
\end{aligned}
\tag{C3}
$$

We can diagonalize the up squark mass square matrix by the unitary transformation

$$
\tilde{D}^{u\dagger} M^2_{\tilde{u}} \tilde{D}^u = \mathrm{diag}(M^2_{\tilde{u}_1}, M^2_{\tilde{u}_2}, M^2_{\tilde{u}_3}, M^2_{\tilde{u}_4}, M^2_{\tilde{u}_5}, M^2_{\tilde{u}_6}, M^2_{\tilde{u}_7}, M^2_{\tilde{u}_8} M^2_{\tilde{u}_9}, M^2_{\tilde{u}_{10}}). \tag{C4}
$$

[1] R. Golub and K. Lamoreaux, Phys. Rep. **237**, 1 (1994).
[2] W. Bernreuther and M. Suzuki, Rev. Mod. Phys. **63**, 313 (1991); I. I. Y. Bigi and N. G. Uraltsev, Sov. Phys. JETP **73**, 198 (1991); M. J. Booth, arXiv:hep-ph/9301293; M. B. Gavela, A. Le Yaouanc, L. Oliver, O. Pène, J.-C. RaynaL, and T. N. Pham, Phys. Lett. **109B**, 215 (1982); I. B. Khriplovich and A. R. Zhitnitsky, Phys. Lett. **109B**, 490 (1982); E. P. Shabalin, Sov. Phys. Usp. **26**, 297 (1983); I. B. Kriplovich and S. K. Lamoureaux, *CP Violation Without Strangeness*, (Springer-Verlag, Heidelberg, 1997).
[3] T. Ibrahim and P. Nath, Rev. Mod. Phys. **80**, 577 (2008); arXiv:hep-ph/0210251; A. Pilaftsis, arXiv:hep-ph/9908373; M. Pospelov and A. Ritz, Ann. Phys. (Amsterdam) **318**, 119 (2005); J. Engel, M. J. Ramsey-Musolf, and U. van Kolck, Prog. Part. Nucl. Phys. **71**, 21 (2013).
[4] J. L. Hewett *et al.*, arXiv:1205.2671.
[5] F. Hoogeveen, Nucl. Phys. **B341**, 322 (1990).
[6] A. Soni and R. M. Xu, Phys. Rev. Lett. **69**, 33 (1992).
[7] The analysis of Ref. [5] was for the electron, and other EDMs are obtained by scaling as noted in Ref. [6].
[8] H. Georgi, Nucl. Phys. **B156**, 126 (1979); F. Wilczek and A. Zee, Phys. Rev. D **25**, 553 (1982); J. Maalampi, J. T. Peltoniemi, and M. Roos, Phys. Lett. B **220**, 441 (1989); J. Maalampi and M. Roos, Phys. Rep. **186**, 53 (1990); K. S. Babu, I. Gogoladze, P. Nath, and R. M. Syed, Phys. Rev. D **72**, 095011 (2005); **74**, 075004 (2006); **85**, 075002 (2012); P. Nath and R. M. Syed, Phys. Rev. D **81**, 037701 (2010).
[9] C. Liu, Phys. Rev. D **80**, 035004 (2009).
[10] S. P. Martin, Phys. Rev. D **81**, 035004 (2010).
[11] K. S. Babu, I. Gogoladze, M. U. Rehman, and Q. Shafi, Phys. Rev. D **78**, 055017 (2008).
[12] T. Ibrahim and P. Nath, Phys. Rev. D **84**, 015003 (2011).
[13] T. Ibrahim and P. Nath, Phys. Rev. D **82**, 055001 (2010).
[14] T. Ibrahim and P. Nath, Phys. Rev. D **81**, 033007 (2010); **89**, 119902(E) (2014).
[15] T. Ibrahim and P. Nath, Phys. Rev. D **78**, 075013 (2008).
[16] T. Ibrahim and P. Nath, Nucl. Phys. B, Proc. Suppl. **200–202**, 161 (2010).
[17] T. Ibrahim and P. Nath, Phys. Rev. D **87**, 015030 (2013).
[18] T. Ibrahim, A. Itani, and P. Nath, Phys. Rev. D **90**, 055006 (2014).
[19] T. Ibrahim, A. Itani, and P. Nath, Phys. Rev. D **92**, 015003 (2015).
[20] A. Aboubrahim, T. Ibrahim, and P. Nath, Phys. Rev. D **89**, 093016 (2014).
[21] A. Aboubrahim, T. Ibrahim, A. Itani, and P. Nath, Phys. Rev. D **89**, 055009 (2014).
[22] A. Aboubrahim, T. Ibrahim, and P. Nath, Phys. Rev. D **88**, 013019 (2013).
[23] A. Aboubrahim, T. Ibrahim, and P. Nath, Phys. Rev. D **91**, 095017 (2015).
[24] J. Ellis, S. Ferrara, and D. V. Nanopoulos, Phys. Lett. **114B**, 231 (1982); W. Buchmuller and D. Wyler, Phys. Lett. **121B**, 321 (1983); F. del'Aguila, M. B. Gavela, J. A. Grifols, and A. Mendez, Phys. Lett. **126B**, 71 (1983); J. Polchinski and M. B. Wise, Phys. Lett. **125B**, 393 (1983); E. Franco and M. Mangano, Phys. Lett. **135B**, 445 (1984).
[25] P. Nath, Phys. Rev. Lett. **66**, 2565 (1991).

[26] T. Ibrahim and P. Nath, Phys. Lett. B **418**, 98 (1998); Phys. Rev. D **57**, 478 (1998); **58**, 111301 (1998); **61**, 093004 (2000).
[27] T. Falk and K. A. Olive, Phys. Lett. B **439**, 71 (1998); M. Brhlik, G. J. Good, and G. L. Kane, Phys. Rev. D **59**, 115004 (1999).
[28] K. S. Babu, B. Dutta, and R. N. Mohapatra, Phys. Rev. D **61**, 091701 (2000).
[29] D. McKeen, M. Pospelov, and A. Ritz, Phys. Rev. D **87**, 113002 (2013).
[30] T. Moroi and M. Nagai, Phys. Lett. B **723**, 107 (2013).
[31] W. Altmannshofer, R. Harnik, and J. Zupan, J. High Energy Phys. 11 (2013) 202.
[32] M. Dhuria and A. Misra, Phys. Rev. D **90**, 085023 (2014).
[33] A. Manohar and H. Georgi, Nucl. Phys. **B234**, 189 (1984).
[34] C. A. Baker *et al.*, Phys. Rev. Lett. **97**, 131801 (2006).
[35] T. M. Ito, J. Phys. Conf. Ser. **69**, 012037 (2007).
[36] K. A. Olive *et al.* (Particle Data Group), Chin. Phys. C **38**, 090001 (2014).
[37] R. N. Mohapatra, Phys. Scr. **90**, 088004 (2015).